Chapter 2
Traveling Waves in One-Dimensional Excitable Media

We now consider our first example of wave propagation in neural media, namely, the propagation of an action potential along the axon of a neuron. Such a phenomenon can be formulated mathematically in terms of finding a traveling pulse solution of the spatially extended Hodgkin–Huxley equations (1.8) and (1.4). Formally speaking, a traveling wave is a solution of a PDE on an infinite domain that travels at constant velocity and fixed shape. For one-dimensional systems, one can distinguish two types of solitary traveling wave: a traveling front linking a stable resting state to a stable excited state and a traveling pulse that begins and ends at the resting state; see Fig. 2.1. For the Hodgkin–Huxley model, a traveling front would occur if the recovery variable n associated with K^+ channels were frozen; otherwise repolarization ensures that the trailing edge of the wave returns to the resting state. In order to develop the basic theory of wave propagation in one-dimensional excitable media, we will consider a simplified version of the Hodgkin–Huxley equations given by the FitzHugh–Nagumo (FN) equations [192, 446]:

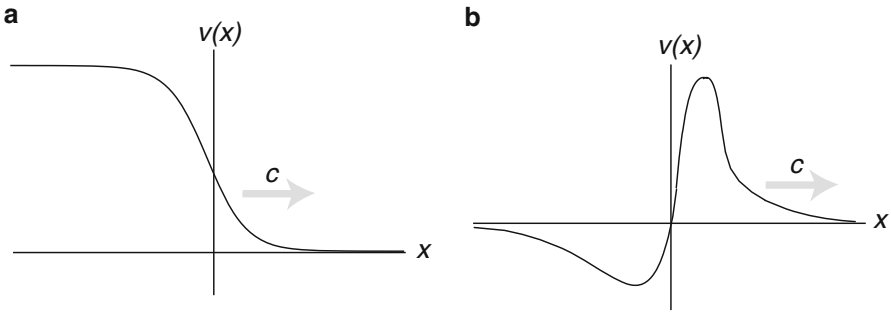

Fig. 2.1 Schematic illustration of (**a**) a traveling front, and (**b**) a traveling pulse

P.C. Bressloff, *Waves in Neural Media: From Single Neurons to Neural Fields*,
Lecture Notes on Mathematical Modelling in the Life Sciences,
DOI 10.1007/978-1-4614-8866-8_2, © Springer Science+Business Media New York 2014

$$\frac{\partial v}{\partial t} = \frac{\partial^2 v}{\partial x^2} + f(v) - w \equiv f(v,w), \tag{2.1a}$$

$$\frac{\partial w}{\partial t} = \varepsilon(v - w) \equiv \varepsilon g(v,w). \tag{2.1b}$$

with $0 < \varepsilon \ll 1$ and

$$f(v) = v(v-a)(1-v). \tag{2.2}$$

Here v represents a fast voltage variable and w is a slow recovery variable. The time and space scales have been non-dimensionalized so that the effective diffusivity of the cable is unity. A number of excellent reviews of waves in excitable systems can be found elsewhere [242, 316, 322, 444].

2.1 Excitable Systems

Before consider traveling wave solutions, it is instructive to consider the excitable behavior of the space-clamped (x-independent) FN model. The space-clamped FN model takes the form of a planar dynamical system

$$\frac{dv}{dt} = f(v,w), \tag{2.3a}$$

$$\frac{dw}{dt} = \varepsilon g(v,w). \tag{2.3b}$$

The fast variable has a cubic nullcline (along which $\dot{v} = 0$) and the slow variable has a monotonically increasing nullcline (along which $\dot{w} = 0$). It is assumed that the nullclines have a single intersection point at (v^*, w^*). This corresponds to a fixed point of the system, which we identify with the resting state. A schematic diagram of the phase plane is shown in Fig. 2.2. For a finite range of values of w, there exist three solutions $v = v(w)$ of the equation $f(v,w) = 0$, which we denote by $V_-(w), V_0(w)$, and $V_+(w)$. Whenever these solutions coexist, we have the ordering $V_-(w) \le V_0(w) \le V_+(w)$. Let W_* denote the minimal value of w for which $V_-(w)$ exists, and let W^* denote the maximal value of w for which $V_+(w)$ exists.

First, suppose that the fixed point is located on the left-hand branch close to the minimum of the cubic. It is straightforward to show that the fixed point is linearly stable by evaluating the eigenvalues of the corresponding Jacobian. Moreover, the system is excitable in the sense that sufficiently large perturbations of the resting state result in a time-dependent trajectory taking a prolonged excursion through state space before returning to the resting state; see Fig. 2.3. Such a trajectory rapidly transitions to the right branch V_+, after which it slowly moves upward in a neighborhood of the branch before reaching the maximum. It then rapidly transitions back to the left branch V_- followed by a slow returns to the resting state along this branch. The time-dependent plot of the variable v can be interpreted as an action potential. Since the resting state is linearly stable, small perturbations simply result in small

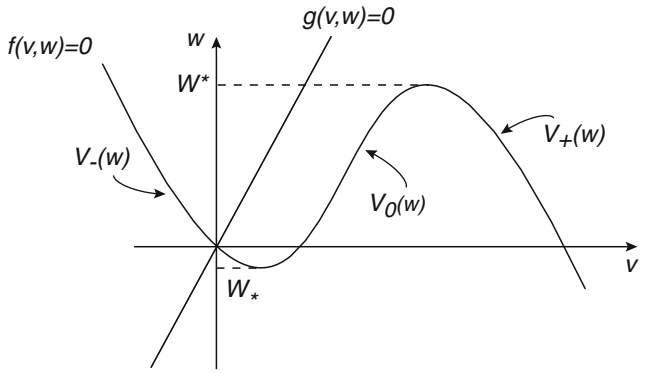

Fig. 2.2 Schematic diagram of the phase plane for the FitzHugh–Nagumo equations

excursions that decay exponentially in time. Hence, there is effectively a threshold phenomenon in which subthreshold perturbations result in a simple return to the resting state, whereas superthreshold perturbations generate an action potential.

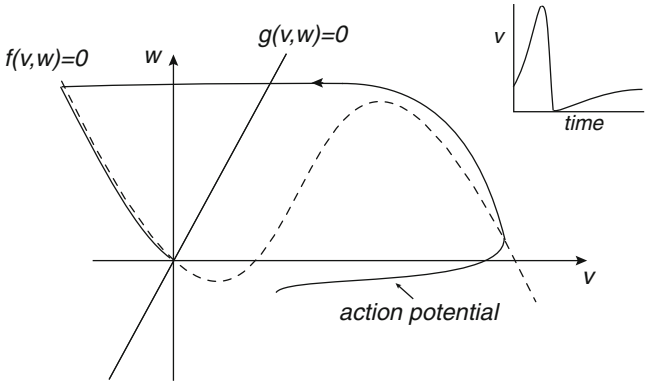

Fig. 2.3 Schematic diagram illustrating the trajectory of a single action potential in the phase plane for the FitzHugh–Nagumo equations. The unique rest point is stable. Inset shows the action potential as a function of time

A more mathematical description of the above events can be developed in terms of singular perturbation theory [242, 322]. Due to the separation of time scales with $\varepsilon \ll 1$, the fast variable v rapidly adjusts whenever it can to maintain the quasi-equilibrium $f(v,w) = 0$. This can be captured by introducing the slow time scale $\tau = \varepsilon t$ such that (2.3) become

$$\varepsilon \frac{dv}{d\tau} = f(v,w), \quad \frac{dw}{d\tau} = g(v,w). \tag{2.4}$$

Now setting $\varepsilon = 0$ and assuming that v is moving along the stable branches $V_\pm(w)$ of $f(v,w) = 0$, the dynamics of the recovery variable reduces to

$$\frac{dw}{d\tau} = g(V_\pm(w), w) \equiv G_\pm(w). \tag{2.5}$$

In the case of rapid transitions between the left and right branches, the dynamics with respect to the fast time scale can be approximated by setting $\varepsilon = 0$ in (2.3),

$$\frac{dv}{dt} = f(v,w), \quad \frac{dw}{dt} = 0. \tag{2.6}$$

Thus, on this time scale, w is constant and v converges to a stable solution of $f(v,w) = 0$. Suppose that the system starts from a superthreshold initial condition (v_0, w_0) such that $v_0 > V_0(w_0)$. After rapidly reaching the right branch, it takes a finite time to reach the upper "knee" of the nullcline $f(v,w)$ and is obtained by integrating (2.5):

$$T_e = \int_{w_0}^{W^*} \frac{dw}{G_+(w)}. \tag{2.7}$$

On the other hand, the time taken to return to the resting state along the left branch is infinite, since $G_-(w)$ vanishes at the fixed point.

It is possible to convert the FN equations from an excitable to an oscillatory regime by adding a constant external current I_{ext} to the right-hand side of the voltage equation in (2.3). For an intermediate range of values of I_{ext} one finds that the fixed point shifts to the middle branch $V_0(w)$ where it is unstable. The fixed point now coexists with a limit cycle, along which the trajectory alternates periodically between the left and right branches, while w varies between W_* and W^*; see Fig. 2.4. The resulting limit cycle behavior with fast jumps alternating with slow dynamics is known as a *relaxation oscillator*. For small ε, the period T of the oscillator is dominated by the times to move along the left and right branches. Hence

$$T = \int_{W_*}^{W^*} \left(\frac{1}{G_+(w)} - \frac{1}{G_-(w)} \right) dw, \tag{2.8}$$

with $G_+ > 0$ and $G_- < 0$.

Another well-known planar model of an excitable neuron is the Morris–Lecar (ML) model [440] (see Eq. (1.28)) which we write in the form

$$\frac{dv}{dt} = a(v) f_{\text{Na}}(v) + w f_{\text{K}}(v) - g(v) \tag{2.9a}$$

$$\frac{dw}{dt} = \frac{w_\infty(v) - w}{\tau_w(v)}, \tag{2.9b}$$

where $f_i(v) = g_i(v_i - v)$ and w represents the fraction of open K^+ channels. The fraction of Na^+ channels (or Ca^{2+} channels in the original formulation of the model) is assumed to be in quasi steady state. Again we can analyze the generation of action

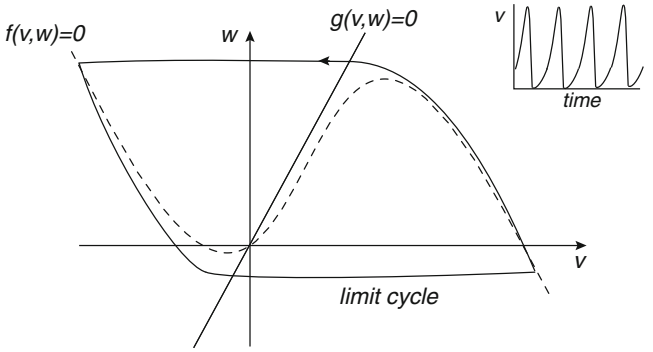

Fig. 2.4 Schematic diagram illustrating the trajectory of a globally stable periodic orbit in the phase plane for the FitzHugh–Nagumo equations. The unique rest point is unstable. Inset shows the periodic orbit as a function of time

potentials using a slow/fast analysis of the deterministic system. However, it turns out that this adiabatic approximation breaks down when stochastic fluctuations in the opening and closing of K^+ channels are taken into account. This can be established by considering a stochastic version of the ML model [456] consisting of N sodium and M potassium channels (see also Sect. 1.5):

$$\frac{dv}{dt} = F(v,m,n) \equiv \frac{n}{N} f_{\rm Na}(v) + \frac{m}{M} f_{\rm K}(v) - g(v). \tag{2.10}$$

We assume that each channel can either be open or closed and can switch between each state according to the kinetic scheme

$$C \underset{\beta_i(v)}{\overset{\alpha_i(v)}{\rightleftarrows}} O, \quad i = {\rm Na},\ {\rm K}, \tag{2.11}$$

The Na^+ channels open and close rapidly relative to the voltage and K^+ dynamics. The probability density function $p(v,m,n,t)$ of the resulting stochastic hybrid system (see Sect. 1.6) evolves according to the differential Chapman–Kolmogorov (CK) equation,

$$\frac{\partial p}{\partial t} = -\frac{\partial (Fp)}{\partial v} + \mathbb{L}_{\rm K} p + \mathbb{L}_{\rm Na} p. \tag{2.12}$$

The jump operators $\mathbb{L}_j$, $j = {\rm Na}, {\rm K}$, are defined according to

$$\mathbb{L}_j = (\mathbb{E}_n^- - 1)\omega_j^+(n,v) + (\mathbb{E}_n^+ - 1)\omega_j^-(n,v), \tag{2.13}$$

with $\mathbb{E}_n^{\pm} f(n) = f(n \pm 1)$, $\omega_j^-(n,v) = n\beta_j(v)$ and $\omega_j^+(n,v) = (N-n)\alpha_j(v)$.

Introducing the small parameter ε with $\alpha_{\rm Na}, \beta_{\rm Na}, M = \mathcal{O}(1/\varepsilon)$, one can extend the WKB approximation method of Sect. 1.6 to analyze noise-induced transitions in the phase plane [456]. The WKB potential Φ can be interpreted as the action of an effective Hamiltonian dynamical system whose solutions determine charac-

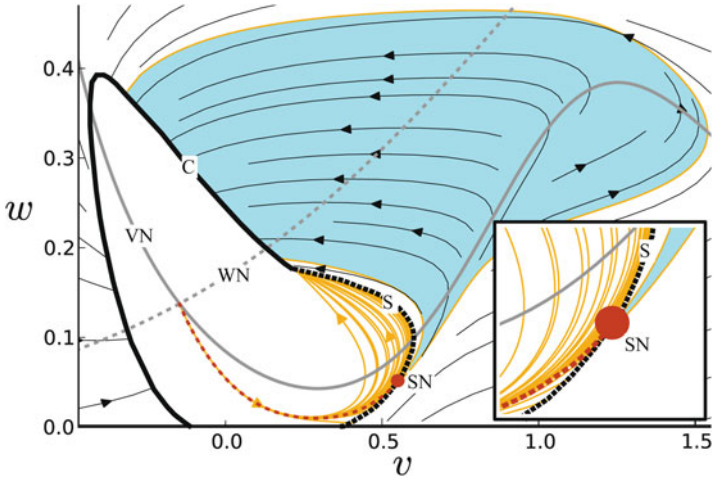

Fig. 2.5 Illustration of spontaneous action potentials (SAPs) for the stochastic ML model (2.10) with a finite number of sodium and potassium ion channels [456]. Orange curves are SAP trajectories, shown until they reach the effective metastable separatrix (S). The dashed red curve is a SAP that reaches S near the metastable saddle (SN). All of the SAP trajectories in the shaded region—containing the most probable, observable SAP trajectories—are visually indistinguishable from the dashed red line before crossing S. Deterministic trajectories are shown as black streamlines. Also shown are a caustic (C), caustic formation point (CP), v nullcline (VN), and w nullcline (WN). Parameter values are $N = M = 10$ and $\varepsilon = 0.1$

teristic paths in the phase plane (see also Sect. 4.4). The latter correspond to the paths a stochastic trajectory is most likely to follow during a metastable transition (i.e., a path of maximum likelihood [160]). Based on the fast/slow analysis of the deterministic system (2.9), one might expect w to be approximately constant along a stochastic trajectory that jumps between the left and right branches of the voltage nullcline, since the K^+ channels open and close slowly. In fact this does not hold for spontaneous action potentials arising from K^+ channel fluctuations [456] (see Fig. 2.5), which is in contrast to the effects of noise in the voltage or fast sodium channels. In general, it is difficult to solve FPT problems in more than one dimension. In the case of a metastable state with a well-defined basin of attraction, one has to calculate the MFPT to cross the separatrices forming the boundary of the basin of attraction. There is an additional level of complexity for an excitable system, due to the fact that there is no well-defined deterministic separatrix. Interestingly, as illustrated in Fig. 2.5, the stochastic ML model has an effective separatrix that any stochastic trajectory has to cross in order to generate a stochastic action potential [456]; see also [327]. Another commonly observed feature of the WKB approximation in two or more dimensions is the formation of caustics, where characteristic projections of the Hamiltonian intersect. There is now quite an extensive literature on the effects of noise in excitable systems, as reviewed in [383]. Most of these studies consider extrinsic Gaussian noise in the voltage dynamics and phenomena such as stochastic and coherence resonance. In Sect. 2.6 we will consider the effects of

Gaussian noise on wave propagation in a spatially extended excitable system. One can motivate this form of noise by considering diffusion approximations of models of stochastic ion channels. However, as the above example shows, certain caution must be exercised when considering such approximations.

Finally, we note that fast/slow decomposition has been applied extensively in recent years to the study of rhythmic activity patterns in single neurons and in synaptically coupled relaxation oscillators (see also Sect. 5). In the latter case, if synapses turn on and off on the fast time scale, then geometric singular perturbation theory can be used to investigate how synaptic inputs modify geometric structures such as null surfaces in the phase spaces of individual neurons, as reviewed by Rubin and Terman [537]; see also Chap. 9 of [173]. Moreover, such methods have been used to study a three-dimensional version of the Hodgkin–Huxley model, in which there is one fast variable and two slow variables [539, 540]. In addition to the transition from excitable to regular oscillatory behavior, as observed in classical relaxation oscillators, the model neuron also exhibits more complex dynamics such as mixed-mode oscillations that are associated with slow action potentials.

2.2 Traveling Fronts in a Scalar Bistable Equation

In the absence of a recovery variable, the FN equations reduce to the so-called scalar bistable equation

$$\frac{\partial v}{\partial t} = \frac{\partial^2 v}{\partial x^2} + f(v), \quad -\infty < x < \infty \tag{2.14}$$

with $f(v)$ given by the cubic (2.2). For such a choice of nonlinearity, the corresponding ODE, $dv/dt = f(v)$, has stable equilibria at $v = 0, 1$ separated by an unstable equilibrium at $x = a$. We define a traveling front solution according to

$$v(x,t) = v(x - ct) = V(\xi), \quad \xi = x - ct \tag{2.15}$$

for some yet to be determined wave speed c, supplemented by asymptotic boundary conditions ensuring that the front links the two stable fixed points of the x-independent system. For concreteness, we take

$$V(\xi) \to 1 \text{ as } \xi \to -\infty, \quad V(\xi) \to 0 \text{ as } \xi \to \infty. \tag{2.16}$$

Substituting the traveling front solution into the bistable Eq. (2.14) yields the ODE

$$V_{\xi\xi} + cV_\xi + f(V) = 0, \tag{2.17}$$

where $V_\xi = dV/d\xi$.

Classical phase-plane analysis can be used to find a traveling front solution by rewriting the second-order equation in the form

$$V_\xi = Z, \quad Z_\xi = -cZ - f(V). \tag{2.18}$$

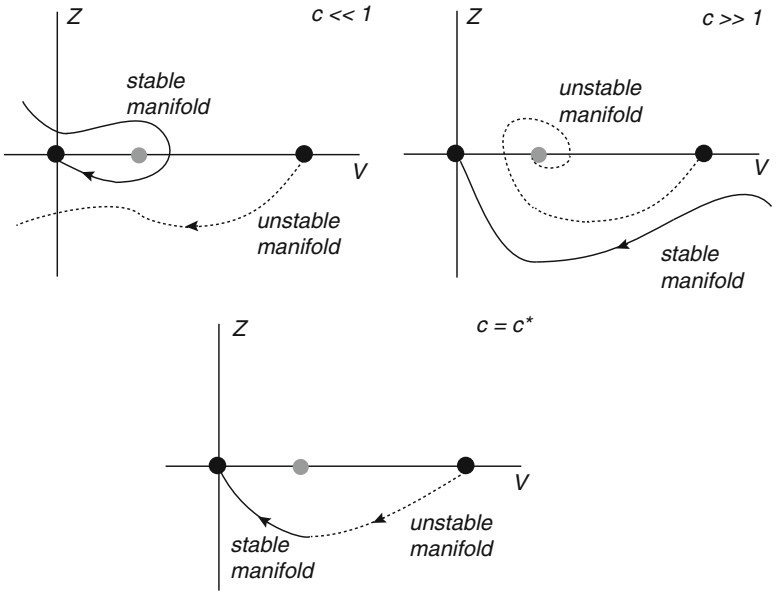

Fig. 2.6 Shooting method for constructing a front solution in the (V,Z) phase plane with $Z = V_\xi$. See text for details

One now has to look for a heteroclinic connection that links the excited state $(V,Z) = (1,0)$ at $\xi \to -\infty$ to the resting state at $\xi \to \infty$. This can be achieved using a geometric argument based on a shooting method, as illustrated in Fig. 2.6. For the sake of illustration, suppose that $0 < a < 1/2$ so that $c > 0$ (see below). First note that irrespective of the speed c, the fixed points $(1,0)$ and $(0,0)$ are saddles, each with one-dimensional stable and unstable manifolds. By looking at trajectories in the phase plane, it is straightforward to see that when $c \ll 1$, the unstable manifold of $(1,0)$ lies below the stable manifold of $(0,0)$ when $0 < V < 1$, whereas the opposite holds when c is very large. Since these manifolds depend continuously on c, it follows that there must exist at least one value of c for which the manifolds cross, and this corresponds to the heteroclinic connection that represents the traveling front solution. It can also be established that this front is unique. A useful formula for determining the sign of the wave speed can be obtained by multiplying both sides of (2.17) by V_ξ and integrating with respect to ξ:

$$\begin{aligned} c\int_{-\infty}^{\infty}(V_\xi)^2 d\xi &= -\int_{-\infty}^{\infty} V_\xi f(V(\xi))d\xi - \int_{-\infty}^{\infty} V_\xi V_{\xi\xi} d\xi, \\ &= \int_0^1 f(V)dV, \end{aligned} \tag{2.19}$$

since $V(\xi)$ is monotone, and $\int_{-\infty}^{\infty} V_\xi V_{\xi\xi} d\xi = \int_{-\infty}^{\infty} \frac{d[V_\xi^2/2]}{d\xi} d\xi = 0$. As the integral on the left-hand side is positive, it follows that the sign of c is determined by the

sign of the area of f between the two stable equilibria. If $0 < a < 1/2$, then the latter is positive and the wave moves to the right, converting the medium from the resting state to the excited state. On the other hand, a left-moving front occurs when $1/2 < a < 1$, converting the medium from the excited state to the resting state. If the negative and positive areas exactly cancel, then the front is stationary.

The numerical construction of the traveling front using a shooting method does not depend on the precise form of f. However, if f is given by the cubic (2.2), then it is possible to construct the front explicitly. That is, we substitute the ansatz $Z = -AV(1-V)$ into (2.17) to obtain the condition $A^2(2V-1) + cA - (V-a) = 0$. Collecting terms linear in V and terms independent of V requires $A = 1/\sqrt{2}$ and $c = (1-2a)/\sqrt{2}$. This immediately establishes that c switches sign at $a = 1/2$. Since $W = V_\xi$, it follows that the corresponding wave profile is

$$V(\xi) = \frac{1}{2}\left[1 - \tanh(\xi/2\sqrt{2})\right].$$

Finally, recall that we have non-dimensionalized the units of space and time in the bistable equation by setting the membrane time and space constants of the cable to unity ($\tau_m = 1, \lambda_m = 1$); see (1.55). Hence, in physical units, the speed of the wave is

$$\hat{c} = \frac{c\lambda_m}{\tau_m} = \frac{c}{2C_m}\sqrt{\frac{d}{R_m R}}, \tag{2.20}$$

where d is the cable diameter. Based on empirical estimates, one finds that $\hat{c} \sim \sqrt{d}\,\mathrm{mm/sec}$. In the case of a squid axon of diameter $d = 500\,\mu\mathrm{m}$, the estimated propagation speed is of around $20\,\mathrm{mm/ms}$.

Another choice of nonlinearity for which an explicit front can be calculated is the piecewise linear function

$$f(v) = -v + H(v-a). \tag{2.21}$$

Substituting into Eq. (2.17) gives

$$V_{\xi\xi} + cV_\xi - V + H(V-a) = 0. \tag{2.22}$$

Translation symmetry of the system means that we are free to choose V to cross the threshold a at $\xi = 0$ so that $V(\xi) > a$ for $\xi < 0$ and $V(\xi) < a$ for $\xi > 0$. Solving the resulting linear equation on either side of the threshold point $\xi = 0$ and imposing the threshold condition $V(0) = a$ yields the explicit solution

$$V(\xi) = \begin{cases} a\mathrm{e}^{\lambda_- \xi}, & \xi > 0 \\ 1 + (a-1)\mathrm{e}^{\lambda_+ \xi}, & \xi < 0, \end{cases} \tag{2.23}$$

where $\lambda_\pm$ are the roots of the characteristic equation $\lambda^2 + c\lambda - 1 = 0$. The wave speed is then obtained by imposing continuity of V_ξ at $\xi = 0$, $(a-1)\lambda_+ = a\lambda_-$, which after rearranging gives

$$c = \frac{1-2a}{\sqrt{a-a^2}}. \tag{2.24}$$

2.3 Traveling Pulses in the FitzHugh–Nagumo Equations

The bistable equation cannot support a traveling pulse solution because there is no recovery variable, that is, it does describe an excitable system. In order to obtain traveling pulse solutions, it is necessary to consider the full FitzHugh–Nagumo equations (2.1). Suppose that the unique fixed point (v^*, w^*) lies on the left-hand branch as in Fig. 2.2. Assume a traveling wave solution of the form $(v(x,t), w(x,t)) = (V(\xi), W(\xi))$ with $\xi = x - ct$ so that (2.1) reduce to the system of ODEs

$$V_{\xi\xi} + cV_\xi + f(V,W) = 0, \tag{2.25a}$$

$$cW_\xi + \varepsilon g(V,W) = 0. \tag{2.25b}$$

These are supplemented by the asymptotic boundary conditions

$$\lim_{\xi \to \pm\infty} (V(\xi), W(\xi)) = (v^*, w^*). \tag{2.26}$$

Mathematically speaking, one needs to find a trajectory in the phase space (V,Z,W) with $Z = V_\xi$ that is homoclinic to the resting state $(v^*, 0, w^*)$. (Although the resting state is stable in the space-clamped system, it is a saddle in the phase plane (V,Z,W) of the spatially extended system.) The existence of such an orbit can be demonstrated using geometric singular perturbation theory [104, 267]. The basic idea is to formally set $\varepsilon = 0$ and construct a singular homoclinic orbit. This will consist of four parts: the jump-up from the resting state to the right branch $V_+(w)$, an active phase along $V_+(w)$, the jump-down to the left branch $V_-(w)$, and a quiescent phase as it returns to the resting state along $V_-(w)$; see Fig. 2.7. Given the existence of a singular homoclinic orbit, one can then prove that such an orbit persists for $\varepsilon > 0$ provided that ε is sufficiently small. In this section we will focus on the construction of the singular solution, exploiting the fact that the jumps take place on a fast spatial scale ξ, whereas the active and quiescent phases occur on a slow spatial scale $z = \varepsilon\xi$.x

In order to analyze the jump-up from the resting state to the active phase, we set $\varepsilon = 0$ in (2.25) to obtain the reduced system

$$V_{\xi\xi} + cV_\xi + f(V,W) = 0, \tag{2.27a}$$

$$W_\xi = 0. \tag{2.27b}$$

Thus the recovery variable is a constant w and V evolves according to the bistable equation

$$V_{\xi\xi} + cV_\xi + f(V,w) = 0, \tag{2.28}$$

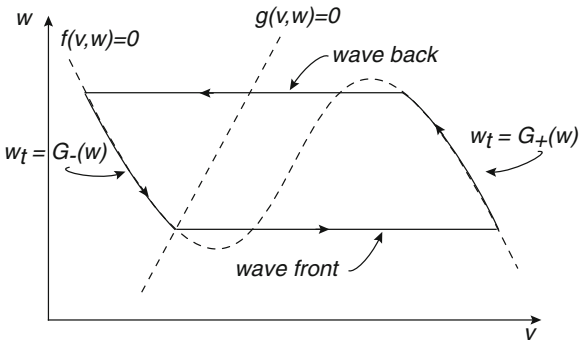

Fig. 2.7 Phase portrait of the fast traveling solitary pulse for the FN equations in the singular limit $\varepsilon \to 0$. The arrow directions are for increasing time (decreasing ξ)

for $f(V,w) = v(v-a)(1-v) - w$. Following Sect. 2.2, we know that for fixed w there exists a unique traveling front solution of (2.28) with associated wave speed $c = c(w)$ that is a heteroclinic connection with $V \to V_L(w)$ as $\xi \to \infty$ and $v \to V_R(w)$ as $\xi \to -\infty$. Moreover,

$$c(w) = \frac{\int_{V_-(w)}^{V_+(w)} f(V,w)dV}{\int_{-\infty}^{\infty} V_\xi^2 d\xi}. \tag{2.29}$$

Setting $w = w^*$ with $V_L(w^*) = v^*$ we obtain the wave speed $c^* = c(w^*)$. Next consider the slow active phase with $c = c^*$. Introducing the slow time scale $z = \varepsilon\xi$ we have

$$\varepsilon^2 V_{zz} + c\varepsilon V_z + f(V,W) = 0, \tag{2.30a}$$
$$cW_z + g(V,W) = 0. \tag{2.30b}$$

Setting $\varepsilon = 0$ then leads to the reduced system

$$f(V,W) = 0, \tag{2.31a}$$
$$W_z = \frac{1}{c^*} g(V,W). \tag{2.31b}$$

Taking the solution $V = V_R(W)$ of $f(V,W) = 0$, it follows that the trajectory moves along the right branch at a rate determined by $G_+(W) = g(V_R(W),W)$.

Now suppose that the trajectory leaves the branch at some value $W = W_d < W^*$ (where W^* is at the maximum of the cubic $f(V,W) = 0$) and jumps back down to the left branch. Similar to the jump-up phase, the recovery variable is constant, and V evolves according to the bistable Eq. (2.28) with $w = W_d$. Again using Sect. 2.2, we can construct a unique traveling wave solution with associated wave speed $c(W_d) < 0$ that is a heteroclinic connection from $V_R(W_d)$ to $V_L(W_d)$. The wave speed is negative, since the jump-down starts from an active state rather than a quiescent

state; it is thus referred to as a wave back. The requirement that the solution be a steadily propagating pulse means that the speeds of the jump-up and jump-down solutions must be the same, which implies that

$$c(w^*) = -c(W_d). \tag{2.32}$$

This condition uniquely determines the transition point W_d. Finally, the trajectory returns to the resting state by moving along the left branch at a rate determined by $G_-(W)/c^*$.

A number of comments are in order. First, from the perspective of matched asymptotics in the slow variable z, the active and quiescent phases correspond to outer solutions that are slowly varying, whereas the jump-up and jump-down phases correspond to transition layers or inner solutions. Denote the wave-front and wave-back solutions by $V_\pm(\xi)$. Matching the inner and outer solutions then leads to the following asymptotic conditions:

$$\begin{aligned}
\lim_{\xi\to-\infty} V_+(\xi) &= V_R(W(0)), \quad W(0) = w^* \\
\lim_{\xi\to\infty} V_+(\xi) &= \lim_{z\to\infty} V_L(W(z)) = v^* \\
\lim_{\xi\to-\infty} V_-(\xi) &= V_L(W(z_T)), \quad W(z_T) = W_d \\
\lim_{\xi\to\infty} V_-(\xi) &= V_R(W(z_T))
\end{aligned}$$

The location z_T where the jump-down occurs is determined from the slow dynamics according to

$$z_T = c^* \int_{w^*}^{W_d} \frac{dW}{G_+(W)} dW. \tag{2.33}$$

One can interpret z_T as the width of the pulse. Second, it may be the case that there is no solution of $c(w^*) = -c(W_d)$ such that $W_d < W^*$. The jump-down transition then occurs at the upper knee, and the solution is referred to as a phase wave, that is, the jump occurs at a time or phase determined solely by the outer dynamics. The wave behavior is then qualitatively different, since the wave can travel at any speed above some minimum, analogous to the well-known Fisher–KPP equation of population genetics [191, 345]; see Sect. 3.3.

2.3.1 Periodic Wave Trains

One of the characteristic features of excitable systems is that they exhibit refractoriness. That is, once the system has responded to a superthreshold stimulus by generating an action potential, there is a refractory period during which no subsequent stimuli can be evoked. From the singular construction of a traveling pulse, the refractory period can be estimated as follows: after the jump-down there is a range of values of the recovery variable, $W_0 \le w \le W_d$ for which the front solution to the

bistable Eq. (2.2) has negative wave speed, $c(w) \leq 0$, with $c(W_0) = 0$. The time taken to reach W_0 from W_d along the left branch is (for fixed x and rescaled time)

$$T_{\text{ref}} = \int_{W_0}^{W_d} \frac{dW}{|G_-(W)|}. \tag{2.34}$$

We can identify T_{ref} as the refractory period. Once excitability has been restored, it is possible to evoke another wave of excitation. However, the speed of the subsequent pulse is expected to be slower due to the residual refractoriness of the system. Now suppose that we periodically initiate action potentials at one end of a semi-infinite cable. This will asymptotically produce a periodic wave train with the time between successive pulses equal to the forcing period T. Assuming that the wave train travels at a speed c, the spatial separation or wavelength of the pulses will be $\lambda = cT$. The speed of the wave train is expected to be smaller than the speed of an isolated pulse due to refractoriness, although this effect should decrease as T increases. In other words, there exists a dispersion curve $c = c(T)$ with $c(T)$, a monotonically increasing function of T.

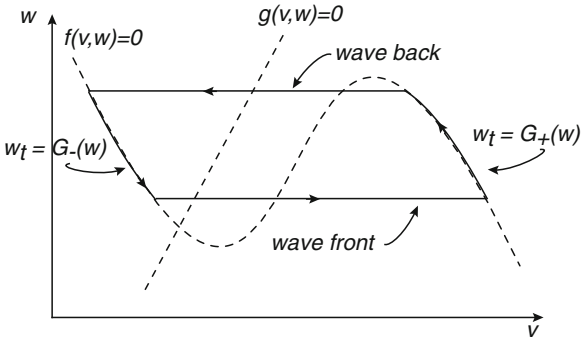

Fig. 2.8 Phase portrait for the fast periodic wave train for the FN equations in the singular limit $\varepsilon \to 0$

It is possible to estimate the dispersion curve for the FitzHugh–Nagumo equations using the previous singular construction. A periodic wave train consists of an alternating sequence of jump-ups and jump-downs, separated by regions of slow dynamics. A phase portrait for such a solution is shown in Fig. 2.8. The major difference from an isolated pulse (see Fig. 2.7) is that the jump-up occurs before reaching the resting state, with $W = W_P > w_*$. Denoting the corresponding value at the jump-down by W_Q, we require that the speeds of the corresponding wave front and wave back are the same, that is, $c(W_P) = -c(W_Q)$. Since the time taken for the jumps is negligible, the major contributions to the period T come from the time spent traversing the right and left branches:

$$T = \int_{W_P}^{W_Q} \frac{dW}{G_+(W)} + \int_{W_Q}^{W_P} \frac{dW}{G_-(W)}. \tag{2.35}$$

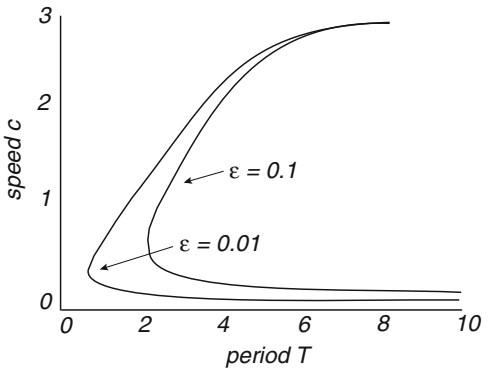

Fig. 2.9 Illustration of typical dispersion curves $c = c(T)$ for T-periodic wave-train solutions of the FN equations. A stable fast branch coexists with an unstable slow branch. They annihilate in a saddle–node bifurcation

Solving for W_Q in terms of W_P using the matching of speeds and inverting the relation $c = c(W_P)$ then generate the dispersion curve $c(T)$. It turns out that the dispersion curve breaks down when the wavelength $\lambda \equiv cT = \mathcal{O}(\varepsilon)$, because the transitional fronts and backs become arbitrarily close together so that it is no longer possible to carry out matched asymptotics. In order to construct the true dispersion curve, it is necessary to carry out a regular perturbation analysis in ε with $c = \mathcal{O}(\varepsilon)$ [156]. One then finds that the dispersion curve consists of two branches that annihilate in a saddle–node bifurcation at $T = T_c$; see Fig 2.9. Hence there are no traveling pulses for $T < T_c$. It can be shown that the upper branch of fast traveling pulses is stable, whereas the lower branch of slow pulses is unstable. (The issue of wave stability will be addressed in Sect. 2.4.) Note that as $T \to \infty$, $c \to c_\infty$ on the upper branch, where c_∞ is the speed of an isolated pulse. Interestingly, c also approaches a finite limit as $T \to \infty$ on the lower branch, suggesting that there also exists a slow unstable isolated pulse; this is indeed found to be the case.

2.3.2 Kinematics

It is also possible to have wave trains consisting of action potentials that are irregularly spaced and move at different speeds. Rinzel and Maginu [523] developed a kinematic theory of wave propagation that uses the dispersion relation to determine the instantaneous speed of a pulse. That is, suppose an initial pulse is generated at $x = 0$ at time t_1. The time at which the pulse reaches a given point x will be $T_1(x) = t_1 + x/c_\infty$, where c_∞ is the speed of a solitary pulse. Suppose that a second spike is initiated at $x = 0$ at time t_2. The instantaneous speed of the new pulse at x will depend on the time difference $T_2(x) - T_1(x)$ due to refractoriness. The Rinzel and Maginu approximation is to take the instantaneous speed to be $c(T_2(x) - T_1(x))$, where $c(T)$ is the dispersion curve for a periodic wave train. It then follows that

$$\frac{dT_2(x)}{dx} = \frac{1}{c(T_2(x) - T_1(x))}, \tag{2.36}$$

and the time interval $\phi = T_2(x) - T_1(x)$ between two action potentials initiated at $x = 0$ will evolve in space according to

$$\frac{d\phi}{dx} = \frac{1}{c(\phi)} - \frac{1}{c_\infty} \equiv \Gamma(\phi). \tag{2.37}$$

If the function $\Gamma(\phi)$ has one or more zeroes $\bar{\phi}$, then the phase difference between the two action potentials will lock at $\bar{\phi}$; the phase-locked state will be stable if $\Gamma'(\phi) < 0$. Note the kinematic approximation can be extended to multiple action potentials under the assumption that the instantaneous speed only depends on the relative phase of the preceding action potential. If $T_{n+1}(x)$ is the arrival time of the $n+1$th action potential, then

$$\frac{dT_{n+1}(x)}{dx} = \frac{1}{c(T_{n+1}(x) - T_n(x))}. \tag{2.38}$$

Note that an explicit version of kinematic theory can be derived using the singular solution of the FN equations [322], assuming that recovery always occurs via a phase wave at the value W^*. Suppose that $w_n(x)$ is the value of the recovery variable along the wave front of the nth pulse when it is located at x. The instantaneous speed of the front is thus $c(w_n)$. The time between fronts of successive action potentials is then given by

$$T_{n+1}(x) - T_n(x) = \int_{w_n}^{w^*} \frac{dw}{G_+(w)} + \int_{w_*}^{w_{n+1}} \frac{dw}{G_-(w)}. \tag{2.39}$$

Differentiating both sides with respect to x and using $dT_n/dx = 1/c(w_n)$ yields

$$\frac{1}{G_-(w_{n+1})}\frac{dw_{n+1}}{dx} = \frac{1}{G_-(w_n)}\frac{dw_n}{dx} + \frac{1}{c(w_{n+1})} - \frac{1}{c(w_n)}. \tag{2.40}$$

This generates an iterative equation for $w_n(x)$, which can be solved to determine the speed and arrival time of each successive action potential.

2.4 Wave Stability and Evans Functions

This section requires some basic definitions and results in functional analysis, in particular, with regard to Banach spaces and the spectrum of linear differential operators; see appendix section 2.7.

2.4.1 Stability of Fronts in the Bistable Equation

In order to introduce some of the basic principles of wave stability, let us return to the simple case of the scalar bistable Eq. (2.14). Let $V(\xi)$, $\xi = x - ct$, denote the unique traveling front solution with speed c such that $V(\xi) \to 1$ as $\xi \to -\infty$ and $V(\xi) \to 0$ as $\xi \to \infty$. In order to investigate the linear stability of such a solution, we set

$$v(x,t) = V(\xi) + \phi(\xi,t), \tag{2.41}$$

where ϕ is some small perturbation belonging to an appropriately defined Banach space $\mathscr{B}$ (complete, normed vector space). It is convenient to use the moving coordinate ξ so that we may see how the perturbation evolves in the moving frame of the front. Substituting for v in (2.14) and keeping only terms linear in ϕ gives

$$\frac{\partial \phi}{\partial t} = \mathbb{L}\phi \equiv \frac{\partial^2 \phi}{\partial \xi^2} + c\frac{\partial \phi}{\partial \xi} + f'(V)\phi, \quad \xi \in \mathbb{R}, \quad t > 0. \tag{2.42}$$

Equation (2.42) takes the form of a linear equation with associated linear differential operator $\mathbb{L} : \mathscr{D}(\mathbb{L}) \to \mathscr{B}$ with domain $\mathscr{D}(\mathbb{L}) \subseteq \mathscr{B}$. Determining the linear stability of the front thus reduces to the problem of calculating the spectrum $\sigma(\mathbb{L})$ of $\mathbb{L}$. That is, the front will be asymptotically stable if $\|\phi\| \to 0$ as $t \to \infty$ for all $\phi \in \mathscr{B}$, with $\|\cdot\|$ the norm on $\mathscr{B}$. This is guaranteed if $\sigma(\mathbb{L})$ lies strictly in the left-hand side of the complex plane, that is, there exists $\beta > 0$ such that $Re(\lambda) \leq -\beta$ for all $\lambda \in \sigma(\mathbb{L})$. The longtime asymptotics is then $\|\phi\| \sim \mathrm{e}^{-\beta t}$. However, differentiating both sides of (2.17) with respect to ξ gives

$$V_{\xi\xi\xi} + cV_{\xi\xi} + f'(V)V_\xi \equiv \mathbb{L}V_\xi = 0,$$

which implies that zero is an eigenvalue of $\mathbb{L}$ with associated eigenfunction V_ξ. This is not a major issue, once one notices that V_ξ is the generator of infinitesimal translations of the front solution:

$$V(\xi + h) = V(\xi) + hV_\xi(\xi) + \mathscr{O}(h^2).$$

Hence, such perturbations only cause a phase shift of the original front and can thus be discounted. This motivates defining stability of the solution V in terms of the stability of the family of waves obtained by rigid translations of V. In other words, V is said to be stable if and only if $v(x,t) = V(\xi) + \phi(\xi,t)$ converges to $V(\xi + h)$ for some constant, finite h as $t \to \infty$. This will hold provided that zero is a simple eigenvalue of $\mathbb{L}$ and the remainder of the spectrum lies in a half-space $\{\lambda, Re(\lambda) \leq -\beta\}$ for some real $\beta > 0$. It is important to note that the spectrum of $\mathbb{L}$ will depend on the choice of Banach space $\mathscr{B}$. Restricting the class of admissible functions can push the spectrum to the left-half complex plane. However, this may exclude classes of perturbations that are physically relevant. A common choice is thus $L^2(\mathbb{R})$, which includes all normalizable, continuous functions on $\mathbb{R}$ with respect to the L_2 norm:

$$\|\phi\| = \int_{-\infty}^{\infty} |\phi(\xi)|^2 d\xi < \infty.$$

We now turn to the spectrum of the differential operator appearing in (2.42). As explained in appendix section 2.7, $\sigma(\mathbb{L})$ consists of isolated eigenvalues of finite multiplicity combined with the essential spectrum, which includes any continuous and residual spectrum. $\mathbb{L}$ is of the general form of the second-order operator considered in appendix section 2.7 (see (2.106)) with constant coefficient $p = c$ and x-dependent coefficient $q(x) = f'(V(x))$. Moreover, $q(x) \to q_\pm$ as $x \to \pm\infty$ with $q_+ = f'(0) = -a$ and $q_- = f'(1) = -1 + a$. Since the essential spectrum is located to the left of the parabolas defined by (2.108), and $q_\pm < 0$, we deduce that the essential spectrum is bounded to the left of $Re(\lambda) = \min\{-a, a-1\}$ and thus does not contribute to any instabilities. The stability of the front thus depends on the eigenvalues λ of $\mathbb{L}$, where

$$\mathbb{L}\phi \equiv \phi_{\xi\xi} + c\phi_\xi + f'(V)\phi = \lambda\phi, \tag{2.43}$$

with $\phi \in L^2(\mathbb{R})$. Suppose that $Re(\lambda) \geq 0$ so $\phi(\xi) \sim \mathrm{e}^{-\beta\xi}$ as $\xi \to \infty$ with $\beta \geq c$. (This follows from noting $f'(V) \to -a$ as $\xi \to \infty$ and analyzing the resulting constant-coefficient characteristic equation.) Performing the change of variables $\psi(\xi) = \phi(\xi)\mathrm{e}^{c\xi/2}$ yields the modified eigenvalue problem

$$\mathbb{L}_1\psi \equiv \psi_{\xi\xi} + \left(f'(V) - \frac{c^2}{4}\right)\psi = \lambda\psi, \tag{2.44}$$

with $\psi \in L^2(\mathbb{R})$, since it also decays exponentially as $|\xi| \to \infty$. The useful feature of the modified operator is that it is self-adjoint, implying that any eigenvalues in the right-half complex plane are real. Multiplying both sides of the self-adjoint eigenvalue Eq. (2.44) by ψ and integrating over $\mathbb{R}$, we have

$$\lambda \int_{-\infty}^{\infty} \psi^2 d\xi = -\int_{-\infty}^{\infty} \left[\psi_\xi^2 - \left(f'(V) - \frac{c^2}{4}\right)\psi^2\right] d\xi. \tag{2.45}$$

Recall that V_ξ is an eigenfunction of $\mathbb{L}$ with $\lambda = 0$, so that if $\Phi(\xi) = V_\xi(\xi)e^{c\xi/2}$, then $\Phi_{\xi\xi} + (f'(\psi) - c^2/4)\Phi = 0$. Hence, (2.45) can be rewritten as

$$\begin{aligned}
\lambda \int_{-\infty}^{\infty} \psi^2 d\xi &= -\int_{-\infty}^{\infty} \left[\psi_\xi^2 + \frac{\Phi_{\xi\xi}\psi^2}{\Phi}\right] d\xi \\
&= -\int_{-\infty}^{\infty} \left[\psi_\xi^2 - \frac{2\psi\psi_\xi\Phi_\xi}{\Phi} + \frac{\Phi_\xi^2\psi^2}{\Phi^2}\right] d\xi \\
&= -\int_{-\infty}^{\infty} \Phi^2 \left(\frac{d}{d\xi}(\psi/\Phi)\right)^2 d\xi.
\end{aligned}$$

This last result implies that $\lambda \leq 0$, and if $\lambda = 0$, then $\psi \sim \Phi = V_\xi$. We conclude that there are no eigenvalues in the right-half complex plane and $\lambda = 0$ is a simple eigenvalue. Thus the traveling front of the scalar bistable equation is stable.

2.4.2 The Evans Function

Determining the stability of traveling pulse solutions of the FN equations (2.1) or the Hodgkin–Huxley equations (1.8) is much more complicated. One general result, however, is that the discrete spectrum of the differential operator obtained by linearizing about a traveling wave solution may be associated with the zeros of a complex analytic function known as the Evans function. Indeed, Evans [177] originally developed the formalism within the context of the stability of solitary pulses in Hodgkin–Huxley-type equations for action potential propagation. Since then, the Evans function construction has been extended to a wide range of PDEs; see the review [551]. The basic construction of the Evans function can be illustrated relatively easily by considering a higher-dimensional version of the bistable equation [173].

Consider a general class of reaction–diffusion equations of the form

$$\frac{\partial u}{\partial t} = D\frac{\partial^2 u}{\partial x^2} + F(u), \tag{2.46}$$

where $u(x,t) \in \mathbb{R}^N$ and $F : \mathbb{R}^N \to \mathbb{R}^N$. Moreover, D is assumed to be a diagonal matrix with positive definite entries corresponding to the diffusion coefficients of the various component fields. Suppose that the system exhibits bistability, that is, there are two stable fixed points $u = u_j$, $j = 1,2$, with $F(u_j) = 0$. We will assume that there exists a traveling front solution $U(\xi)$ with speed c that connects u_1 and u_2. Linearizing about the wave solution along identical lines to the scalar case by setting $u(x,t) = U(\xi) + p(\xi)e^{\lambda t}$ leads to the eigenvalue problem

$$\mathbb{L}p \equiv Dp_{\xi\xi} + cp_\xi + \partial F(U)p = \lambda p, \tag{2.47}$$

where $\partial F(U)$ denotes the matrix with components $\partial F_i/\partial U_j$. It is convenient to rewrite this as a system of $2N$ first-order equations

$$\begin{pmatrix} p_\xi \\ q_\xi \end{pmatrix} = \begin{pmatrix} 0 & I_n \\ D^{-1}(\lambda - \partial F(U)) & -cD^{-1} \end{pmatrix} \begin{pmatrix} p \\ q \end{pmatrix}. \tag{2.48}$$

Any eigensolution of this equation must satisfy the asymptotic conditions

$$\lim_{\xi \to \pm\infty} (p(\xi), q(\xi)) = (0,0).$$

Setting $z = (p,q)^T \in \mathbb{R}^n$, $n = 2N$, the associated ODE takes the general form

$$\mathscr{T}(\lambda)z(\xi) \equiv \frac{dz}{d\xi} - A(\xi;\lambda)z = 0, \tag{2.49}$$

with $A(\xi;\lambda) = A(\xi) + \lambda B(\xi)$. Thus we have a family of linear operators $\mathscr{T}(\lambda) : \mathscr{D} \to \mathscr{B}$ parameterized by λ. We take $\mathscr{B} = L^2(\mathbb{R}, \mathbb{R}^n)$ and $\mathscr{D}$ to be the space of admissible functions such that $z \in \mathscr{B}, \mathscr{T}(\lambda)z \in \mathscr{B}$. The basic form of the linear Eq. (2.49) holds for a wide range of PDEs supporting solitary traveling waves [551]. The discrete spectrum of the operator $\mathbb{L}$ thus corresponds to the values of λ for which $\mathscr{T}(\lambda)$ is not invertible.

An important concept for analyzing (2.49) is that of *exponential dichotomies*. First, consider the linear constant-coefficient equation

$$\frac{dz}{d\xi} = A(\lambda)z, \tag{2.50}$$

for which $A(\lambda)$ is independent of ξ. Suppose that the matrix $A(\lambda)$ is hyperbolic, that is, all its eigenvalues have nonzero real part. We can then decompose $\mathbb{R}^n$ (or its complexification) as

$$\mathbb{R}^n = E_s(\lambda) \oplus E_u(\lambda),$$

where $E_{s,u}(\lambda)$ are the generalized stable and unstable eigenspaces of the matrix $A(\lambda)$. Thus E_s is spanned by $n_+(\lambda)$ eigenfunctions that decay exponentially as $\xi \to \infty$ and E_u is spanned by $n_-(\lambda)$ eigenfunctions that decay exponentially as $\xi \to -\infty$ with $n_+(\lambda) + n_-(\lambda) = n$. The notion of exponential dichotomies can now be extended to (2.49) by noting that

$$\lim_{\xi \to \pm\infty} A(\xi;\lambda) \to A_\pm(\lambda) \tag{2.51}$$

where $A_\pm$ correspond to the matrix appearing in (2.48) in the limits $U(\xi) \to u_1$ and $U(\xi) \to u_2$, respectively. Moreover, the spectral properties of $\mathscr{T}(\lambda)$ can be expressed in terms of these exponential dichotomies. We summarize the main results below:

- Equation (2.49) is said to have an exponential dichotomy on $\mathbb{R}^+$ if and only if the matrix $A_+(\lambda)$ is hyperbolic. Let $\mathscr{V}_+(\lambda)$ denote the linear subspace spanned by solutions of (2.49) that decay as $\xi \to \infty$. The codimension of $\mathscr{V}_+(\lambda)$ is defined to be the Morse index $i_+(\lambda)$ of the exponential dichotomy on $\mathbb{R}^+$, and $i_+(\lambda) = \dim E_u^+(\lambda)$.
- Equation (2.49) is said to have an exponential dichotomy on $\mathbb{R}^-$ if and only if the matrix $A_-(\lambda)$ is hyperbolic. Let $\mathscr{V}_-(\lambda)$ denote the linear subspace spanned by solutions of (2.49) that decay as $\xi \to -\infty$. The dimension of $\mathscr{V}_-(\lambda)$ is defined to be the Morse index $i_-(\lambda)$ of the exponential dichotomy on $\mathbb{R}^-$, and $i_-(\lambda) = \dim E_u^-(\lambda)$.
- λ is in the discrete spectrum if and only if $A_\pm(\lambda)$ are both hyperbolic with the same Morse index $i_+(\lambda) = i_-(\lambda)$ such that $\mathscr{V}_+(\lambda) \cap \mathscr{V}_-(\lambda) \neq \{0\}$.
- λ is in the essential spectrum if either at least one of the two asymptotic matrices $A_\pm(\lambda)$ is not hyperbolic or else if both are hyperbolic but their Morse indices differ.

In most applications the essential spectrum Σ_{ess} lies in the left-half complex plane and thus does not contribute to instabilities of a wave solution. Therefore, suppose that $\lambda \notin \Sigma_{\text{ess}}$. It then follows that $i_+(\lambda) = i_-(\lambda) = k$, say. (For the multicomponent bistable equation $k = N = n/2$.) In order to construct the Evans function, introduce a basis for the subspaces $\mathscr{V}_\pm(\lambda)$ according to

$$\mathscr{V}_-(\lambda) = \text{span}\{Q_1^-, Q_2^-, \ldots, Q_k^-\}, \quad \mathscr{V}_+(\lambda) = \text{span}\{Q_1^+, Q_2^+, \ldots, Q_{n-k}^+\}$$

where each $Q_j^\pm(\xi)$ is an n-dimensional basis vector. Now form the $n \times n$ matrix $\mathscr{M}(\xi)$, in which the first k columns are given by the vectors $Q_j^-(\xi)$, $j = 1, \ldots, k$, and the next $n-k$ columns are given by Q_j^+, $j = 1, \ldots, n-k$. The Evans function is then defined according to

$$\mathscr{E}(\lambda) = \det \mathscr{M}(\xi_0), \tag{2.52}$$

for an arbitrary point ξ_0 which can be taken to be zero. The Evans function has a number of important properties. First, λ is an eigenvalue if and only if $\mathscr{E}(\lambda) = 0$. Second, if λ is a zero of $\mathscr{E}(\lambda)$, then the order of this zero is equal to the algebraic multiplicity of λ viewed as an eigenvalue. Third, the Evans function is analytic. The first property is simple to establish. For $\mathscr{E}(\lambda) = 0$ if and only if $\det \mathscr{M}(\xi_0) = 0$, and the latter holds if and only if there exist constant coefficients c_i^+, c_j^- such that

$$\sum_{j=1}^{k} c_j^- Q_j^-(\xi_0) + \sum_{i=1}^{n-k} c_i^+ Q_i^+(\xi_0) = 0,$$

that is,

$$\sum_{j=1}^{k} c_j^- Q_j^-(\xi_0) = -\sum_{i=1}^{n-k} c_i^+ Q_i^+(\xi_0).$$

Hence, λ is a zero of $\mathscr{E}(\lambda)$ if and only if $\mathscr{V}_+(\lambda)$ and $\mathscr{V}_-(\lambda)$ have a nonzero intersection, which means that λ is an eigenvalue, since the corresponding eigensolution decays at both $\xi = \infty$ and $\xi = -\infty$. Finally, note that one of the powerful features of the Evans function construction is that it can be applied to a wide variety of wave phenomena beyond fronts, including pulses, periodic wave trains, and multi-bump pulses [551]. In a sense, a single pulse is a special case of a front, since the exponential dichotomies on $\mathbb{R}^+$ and R^- are the same, that is,

$$\lim_{\xi \to \pm\infty} A(\xi; \lambda) \to A_0(\lambda),$$

with $A_0(\lambda)$ evaluated at the same resting state.

Finally, a word of caution: linear stability does not necessarily imply nonlinear stability. When considering perturbations about a traveling wave solution of a nonlinear PDE, $p(x,t) = u(x,t) - U(\xi)$, one can decompose the PDE as

$$\frac{\partial p}{\partial t} = \mathbb{L}p + \mathscr{N}(p), \tag{2.53}$$

where $\mathcal{N}(p) = \mathcal{O}(|p|^2)$. Determining linear stability of the traveling wave in terms of the spectrum $\sigma(\mathbb{L})$ assumes that the perturbation p remains small with respect to the given norm. A challenging mathematical problem is determining whether or not this is true. In the simpler case of ODEs one can use the stable manifold the-

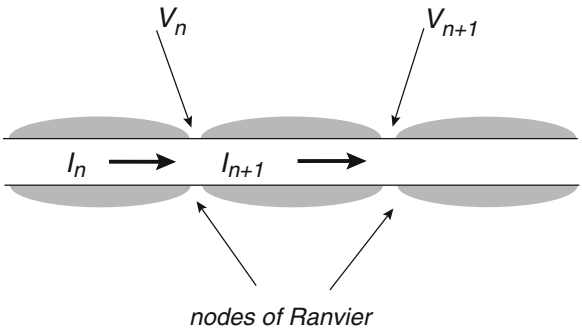

Fig. 2.10 Schematic diagram of a myelinated axon. Currents in myelinated region are confined to the axial direction. Potentials at the nodes are governed by active currents

orem to show that linear (in)stability implies nonlinear (in)stability in the case of hyperbolic fixed points. In the case of non-hyperbolic fixed points one has to use the center manifold theorem and bifurcation theory. A number of techniques have been used to study nonlinear stability of traveling waves, including center manifold reductions, Lyapunov functionals, and energy methods [551]. For example, the nonlinear stability of traveling wave solutions of the reaction–diffusion system (2.46) can be proven using a center manifold reduction. Nonlinear stability theory is also important if one wishes to determine what happens when a traveling wave becomes unstable, since perturbations grow and the linear approximation breaks down.

2.5 Myelinated Axons and Discrete Diffusion

Many vertebrate axons are coated with a lipid material called *myelin*, which is made up of the membranes of *glial cells* (see Sect. 4.5) that wrap around the axon many times to form a thick insulating layer. This wrapping increases the effective membrane resistance and decreases the membrane capacitance by a factor of around 100. At regularly spaced intervals the axon is exposed to the extracellular medium at the so-called nodes of Ranvier, where there is a high density of sodium channels; see Fig. 2.10. The length L of myelin sheath between successive nodes is typically 1–2 mm, and the width l of a single node of Ranvier is around 1 µm. Propagation of an action potential along a myelinated axon is considerably faster than along a nonmyelinated axon. In terms of the cable equation, this can be understood as consequence of the fact that the transmembrane currents in the myelinated sections are

negligible so that the myelinated sheath acts like a simple resistor. In effect, the action potential does not propagate continuously along the axon but rather jumps from node to node as a saltatory (leaping) wave.

Wave propagation along a myelinated axon can be modeled by spatially discretizing the diffusion term in the spatially extended Hodgkin–Huxley model (1.8). Suppose that the membrane voltage does not vary within each node of Ranvier, that is, the nodes are isopotential and denote the voltage of the nth node by V_n. Treating each myelin sheath as a pure Ohmic resistor with resistance rL, where r is the intracellular resistance per unit length, the axial current between nodes n and $n+1$ is

$$I_{n+1} = -\frac{1}{rL}(V_{n+1} - V_n). \tag{2.54}$$

Conservation of current at the nth node of Ranvier then implies that the total transmembrane current into the node is

$$2\pi al\left(C_m\frac{\partial V_n}{\partial t} + I_{\text{ion}}\right) = I_n - I_{n+1} = \frac{1}{rL}(V_{n+1} - 2V_n + V_{n-1}), \tag{2.55}$$

where a is the radius of the cable. It follows that

$$\frac{\partial V_n}{\partial t} = -\hat{I}_{\text{ion}} + D(V_{n+1} - 2V_n + V_{n-1}), \tag{2.56}$$

with coupling coefficient

$$D = \frac{R_m}{(2\pi ar)lL\tau_m} = \frac{\lambda_m^2}{lL\tau_m}.$$

We have used $R = \pi a^2 r$, $\tau_m = R_m C_m$ and $\lambda_m = (R_m a/2R)^{1/2}$; see Sect. 1.4.1.

2.5.1 The Discrete Bistable Equation

In order to investigate the effects of myelination on propagation speed, let us consider the simpler case of the spatially discrete bistable equation

$$\frac{\partial V_n}{\partial t} = f(V_n) + D(V_{n+1} - 2V_n + V_{n-1}), \tag{2.57}$$

where $f(V) = V(V-a)(1-V)$. Proving the existence of traveling wave solutions of (2.57) is nontrivial [699]. However, assuming that such a solution does exist, one can use perturbation methods to estimate the wave speed [317, 321]. A traveling wave solution is defined according to the iterative relationship $V_{n+1}(t) = V_n(t+\tau_d)$ where τ_d represents the time delay for the wave to jump between successive nodes. The corresponding invariant wave profile $\Phi(t)$ satisfies a delay differential equation that is obtained by substituting $V_n(t) = \Phi(t)$ into (2.57):

$$\frac{d\Phi}{dt} = D(\Phi(t-\tau_d) - 2\Phi(t) + \Phi(t+\tau_d)) + f(\Phi(t)). \tag{2.58}$$

Suppose that we fix the time units by setting $\tau_m = 1$. If the function $\Phi(t)$ is sufficiently smooth and τ_d is sufficiently small, then we can expand $\Phi(t \pm \tau_d)$ as a Taylor series in τ_d. Keeping only terms up to τ_d^2 yields the leading-order equation

$$D\tau_d^2 \Phi_{tt} - \Phi_t + f(\Phi) = 0. \tag{2.59}$$

This is identical in form to the bistable Eq. (2.17) for a traveling front of (dimensionless) wave speed c, provided that we set $\xi = -ct$ and $D\tau_d^2 = c^{-2}$. It follows that $\Phi(-\xi/c)$ is the traveling front solution of the continuous bistable equation and $c = (1-2a)/\sqrt{2}$. The wave speed of the saltatory wave (in physical time units) is then

$$\hat{c} = \frac{L+l}{\tau_d} = (L+l)c\sqrt{\frac{D}{\tau_m}} = \frac{L+l}{\sqrt{lL}}\left(\frac{c\lambda_m}{\tau_m}\right). \tag{2.60}$$

Comparison with (2.20) shows that myelination increases wave speed by a factor $(L+l)/\sqrt{lL} \approx 10$ assuming that $L \approx 100l$.

Higher-order corrections to the wave speed can be determined using regular perturbation theory [317, 321]. Thus, in terms of the small parameter $\varepsilon = D^{-1}$, we introduce the series expansions (with $\tau_m = 1$)

$$\Phi(t) = \Phi_0(t) + \varepsilon\Phi_1(t) + \ldots, \quad {\tau_d}^2 = \frac{\varepsilon}{c^2} + \varepsilon^2\tau_1 + \ldots \tag{2.61}$$

Substituting into the discrete bistable Eq. (2.58) and collecting terms of equal powers in ε yields a hierarchy of equations for Φ_n, with Φ_0 satisfying (2.59) for $D\tau_d^2 = c^{-2}$, and

$$\mathbb{L}\Phi_1 \equiv \frac{1}{c^2}\Phi_1'' - \Phi_1' + f'(\Phi_0)\Phi_1 = -\frac{\Phi_0^{(4)}}{12c^4} - \tau_1\Phi_0''. \tag{2.62}$$

Here $\mathbb{L}$ denotes a linear differential operator acting on the space $L^2(\mathbb{R})$ of square-integrable function on $\mathbb{R}$. The operator $\mathbb{L}$ is not invertible, since $\mathbb{L}\Phi_0' = 0$, which follows from differentiating (2.58) with respect to t. (A similar operator arose in our discussion of wave stability in Sect. 2.4.) It follows from the Fredholm alternative (see appendix section 2.7) that a solution for Φ_1 exists if and only if the right-hand side of (2.62) is orthogonal to the null-space of the adjoint operator $\mathbb{L}^\dagger$. The latter is

$$\mathbb{L}^\dagger\mathscr{V} = \frac{1}{c^2}\mathscr{V}'' + \mathscr{V}' + f'(\Phi_0)\mathscr{V}, \tag{2.63}$$

which has a one-dimensional null-space spanned by $\mathscr{V}(t) = \mathrm{e}^{-c^2t}\Phi_0'(t)$. We thus have a solvability condition for the leading-order correction τ_1 to the delay:

$$\int_{-\infty}^{\infty} \mathrm{e}^{-c^2t}\Phi_0'(t)\left[\frac{\Phi_0^{(4)}}{12c^4} + \tau_1\Phi_0''\right]dt = 0.$$

Once τ_1 has been determined, the propagation speed is (in physical time units)

$$\hat{c} = c(L+l)\sqrt{\frac{D}{\tau_m}}\left(1 - \frac{\tau_1 c^2}{2D\tau_m} + \mathcal{O}([c^2/D\tau_m]^2)\right). \tag{2.64}$$

2.5.2 Propagation Failure

The above perturbation analysis establishes that for sufficiently large coupling D, there are traveling front solutions that approach the speed of the appropriately scaled continuous model. Another important property of the discrete bistable equation is that if D is sufficiently small, then wave propagation failure occurs, reflecting the fact that there are nontrivial standing front solutions even when $\int_0^1 f(v)dv > 0$ [165, 183, 317, 318]. Here we describe one method for estimating the critical value of coupling D_c below which propagation fail, which has been developed by Keener [318] using averaging theory. The first step is to rewrite the discrete bistable equation in the form

$$(1+g'(x))[v_t - f(v)] = Dv_{xx}, \tag{2.65}$$

where $g(x)$ is the periodic sawtooth function

$$g(x) = \frac{L}{2} - x, \quad 0 < x < L, \quad g(x+nL) = g(x), \tag{2.66}$$

and

$$1 + g'(x) = L\sum_n \delta(x - nL). \tag{2.67}$$

Equation (2.65) implies that $v_{xx} = 0$ between nodes, that is, $v(x,t) = A_n x + B_n$ for $nL < x < (n+1)L$. Matching $v(x,t)$ with $V_n(t)$ and $V_{n+1}(t)$ at both ends shows that $A_n = L^{-1}[V_{n+1} - V_n]$ and hence $v_x((n+1)L,t) = L^{-1}(V_{n+1} - V_n)$. If we now integrate (2.65) over the interval $[nL,(n+1)L)$, then we recover the discrete bistable equation

$$\partial_t V_n - f(V_n) = \frac{D}{L}[v_x((n+1)L,t) - v_x(nL,t)] = D[V_{n+1} - 2V_n + V_{n-1}]. \tag{2.68}$$

In order to proceed, we will smooth out the function $g(x)$ by taking

$$1 + g'(x) = \frac{L}{\sqrt{2\pi\sigma^2}}\sum_n \exp\left(-\frac{(x-nL)^2}{2\sigma^2}\right), \tag{2.69}$$

so that $1 + g'(x) > 0$ for all x. At the end of the calculation we will take the limit $\sigma \to 0$ to recover the sawtooth function. We then have the scalar bistable equation with an inhomogeneous diffusion coefficient,

$$v_t = f(v) + \frac{D}{1+g'(x)}v_{xx}.$$

Following Keener [318], it is convenient to carry out the coordinate transformation $y = y(x) \equiv x + g(x) - L/2$ so that

$$v_t = f(v) + \partial_y \left([1 + g'(x)] \partial_y v \right).$$

If $g(x)$ is a sawtooth-like function, then y is a steplike function with $y = nL$ for $nL < x < (n+1)L$ in the limit $\sigma \to 0$. Hence $1 + g'(y(x)) = \sum_n \delta(y(x) - nL)$ blows up for all $nL < x < (n+1)L$, whereas $1 + g'(y(x)) = 0$ when $x = nL$. That is, $1 + g'(x) = 1/(1 + g'(y(x)))$, so that (after rewriting y as x),

$$v_t = f(v) + \partial_x \left(\frac{D}{1 + g'(x)} v_x \right).$$

Fixing the spatial units by setting $L = 1$ (having already non-dimensionalized time), and using the fact that waves exist for sufficiently large D, we introduce the small dimensionless parameter $\varepsilon = 1/\sqrt{D}$. Rescaling space according to $x \to x/\sqrt{D}$, we finally obtain the modified bistable equation

$$v_t = f(v) + \partial_x \left(\frac{1}{1 + g'(x/\varepsilon)} v_x \right). \tag{2.70}$$

Thus the problem of wave propagation failure for the discrete bistable equation has been reduced to the problem of calculating the mean wave speed $\bar{c}(\varepsilon)$ of a wavelike solution of an inhomogeneous continuous bistable equation and determining how $\bar{c}(\varepsilon)$ vanishes as ε increases (the coupling D decreases).

Equation (2.70) is now in a suitable form to apply the averaging method of Keener [318]; see below. The basic result is that the wavelike solution takes the form

$$v(x,t) = V(x - \phi(t)) + \mathcal{O}(\varepsilon), \tag{2.71}$$

where $V(x)$ is the wave solution in the homogeneous case ($g = 0$). The phase $\phi(t)$ evolves according to

$$\frac{d\phi}{dt} = c - \Phi(\phi/\varepsilon) \tag{2.72}$$

with c the speed of the unmodulated wave,

$$\Phi(\phi/\varepsilon) = \frac{1}{\Lambda} \int_{-\infty}^{\infty} g'([\xi + \phi]/\varepsilon) V''(\xi) V'(\xi) e^{c\xi} d\xi, \tag{2.73}$$

and

$$\Lambda = \int_{-\infty}^{\infty} e^{c\xi} V'(\xi)^2 d\xi. \tag{2.74}$$

Equation (2.72) implies that the solution is not translationally invariant; rather, it moves with a time-dependent velocity ϕ'. If $c - \Phi(\phi/\varepsilon)$ is strictly positive, then $\phi'(t)$ is a positive, periodic function of t with period

$$T = \int_0^{\varepsilon} \frac{d\phi}{c - \Phi(\phi/\varepsilon)}. \tag{2.75}$$

The mean speed of the wave is $\bar{c} = \varepsilon/T$. On the other hand, if $c - \Phi(\phi/\varepsilon)$ vanishes for some ϕ, then propagation failure is expected to occur:

Averaging method for discrete bistable equation. Standard applications of the averaging theorem in dynamical systems theory [248] only apply to structurally stable solutions, whereas traveling wave solutions are not structurally stable. Therefore, it is necessary to consider a modified averaging procedure as outlined by Keener [318, 319]. The first step is to rewrite (2.70) as the second-order system

$$v_x = (1 + g'(x/\varepsilon))u, \quad u_x = v_t - f(v). \tag{2.76}$$

Introducing the exact change of variables $v = w + \varepsilon u g(x/\varepsilon)$ yields the new system

$$w_x = u - \varepsilon u_x g(x/\varepsilon), \quad u_x = w_t + \varepsilon u_t g(x/\varepsilon) - f(w + \varepsilon u g(x/\varepsilon)). \tag{2.77}$$

It can be seen that if we ignore terms of order ε, then the system of equations is independent of x/ε. This lowest-order averaged system reduces to the standard bistable equation, which we know supports a traveling front solution $V(x - ct)$. Including the inhomogeneous factors $g(x/\varepsilon)$ means that the system is no longer translationally invariant. However, we can look for solutions that are in some sense close to a traveling front by going to a traveling coordinate system by setting $\xi = x - \phi(t)$, with

$$w_\xi = u - \varepsilon u_\xi g([\xi + \phi]/\varepsilon) \tag{2.78a}$$

$$u_\xi = -\phi' w_\xi - \varepsilon \phi' u_\xi g([\xi + \phi]/\varepsilon) - f(w + \varepsilon u g([\xi + \phi]/\varepsilon). \tag{2.78b}$$

We now seek a perturbative solution of the form

$$w = w_0(\xi) + \varepsilon w_1(\xi) + \ldots, \quad v(\xi) = v_0(\xi) + \varepsilon v_1(\xi) + \ldots, \quad \phi'(t) = c + \varepsilon \phi_1'(t) + \ldots$$

Substituting into (2.78) and collecting terms of equal powers in ε yields a hierarchy of equations, the first two of which are

$$\partial_\xi w_0 = u_0, \quad \partial_\xi u_0 = -c u_0 - f(w_0), \tag{2.79}$$

which recovers the homogeneous bistable equation for w_0, and

$$\partial_\xi w_1 - u_1 = -(\partial_\xi u_0) g([\xi + \phi]/\varepsilon), \tag{2.80a}$$

$$\partial_\xi u_1 + f'(w_0) w_1 + c u_1 = -\phi_1' u_0 - f'(w_0) u_0 g([\xi + \phi]/\varepsilon). \tag{2.80b}$$

Let us take the solution of the lowest-order equation to be the traveling front solution $V(\xi)$ constructed in Sect. 2.2: $w_0 = V, u_0 = V'$. The next-order system of Eq. (2.80) can be rewritten in the vector form

$$\mathbb{L}\begin{pmatrix} w_1 \\ u_1 \end{pmatrix} = \begin{pmatrix} h_w \\ -\phi_1' V' + h_u \end{pmatrix}, \quad \mathbb{L} = \begin{pmatrix} \partial_\xi & -1 \\ f'(V) & \partial_\xi + c \end{pmatrix}, \tag{2.81}$$

with h_w and h_u determined by inhomogeneous terms on the right-hand side of (2.80a) and (2.80b), respectively. Following our analysis of the linear operator (2.62), we know that the matrix operator appearing in (2.81) has a null-space spanned by (V', V''). Similarly, the adjoint operator

$$\mathbb{L}^\dagger = \begin{pmatrix} -\partial_\xi & f'(w_0) \\ -1 & -\partial_\xi + c \end{pmatrix}$$

has the null vector $e^{c\xi}(-V'',V')$. Hence, applying the Fredholm alternative, we see that $\phi'(t)$ must satisfy

$$\begin{aligned}\phi_1'(t)\int_{-\infty}^{\infty} e^{c\xi}V'(\xi)^2 d\xi &= \int_{-\infty}^{\infty} e^{c\xi}[-V''(\xi)h_w(\xi)+V'(\xi)h_u(\xi)d\xi \\ &= \int_{-\infty}^{\infty} e^{c\xi}[V''(\xi)^2 - f'(V)V'(\xi)^2]g([\xi+\phi]/\varepsilon)d\xi \\ &= \int_{-\infty}^{\infty} g([\xi+\phi]/\varepsilon)\frac{d}{d\xi}\left[V''(\xi)V'(\xi)e^{c\xi}\right]d\xi, \\ &= -\frac{1}{\varepsilon}\int_{-\infty}^{\infty} g'([\xi+\phi]/\varepsilon)V''(\xi)V'(\xi)e^{c\xi}d\xi,\end{aligned}$$

after using $V'''+cV''+f'(V)V'=0$ and performing integration by parts. We thus obtain the phase Eq. (2.72) with $\phi(t)=c+\varepsilon\phi_1(t)$.

It turns out that solving the phase equation in the case of a cubic nonlinearity is rather involved [318]. Therefore, for the sake of illustration, we will consider the simpler case of the piecewise linear function (2.21). There then exists a unique traveling front solution of the homogeneous bistable equation given by (2.23) with corresponding wave speed (2.24). Substituting (2.23) into (2.74) gives

$$\begin{aligned}\Lambda &= (a\lambda_-)^2\int_0^{\infty} e^{c\xi}e^{2\lambda_-\xi}d\xi + ([a-1]\lambda_+)^2\int_{-\infty}^{0} e^{c\xi}e^{2\lambda_+\xi}d\xi \\ &= (a\lambda_-)^2\left[\frac{1}{c+2\lambda_+}-\frac{1}{c+2\lambda_-}\right] \\ &= 2\sqrt{a-a^2}(a-a^2),\end{aligned}$$

where we have used the results $a\lambda_- = (a-1)\lambda_+$,

$$c+2\lambda_\pm = \pm\sqrt{c^2+4} = \frac{\pm 1}{\sqrt{a-a^2}}, \quad \lambda_- = -\frac{1}{2}\left[c+\sqrt{c^2+4}\right] = \frac{a-1}{\sqrt{a-a^2}}.$$

Similarly, substituting (2.23) into (2.73) gives, to leading order in ε,

$$\begin{aligned}\Phi(\phi/\varepsilon) &= \frac{1}{\Lambda}a^2\lambda_-^3\int_0^{\infty} g'([\xi+\phi]/\varepsilon)e^{c\xi}e^{2\lambda_-\xi}d\xi \\ &\quad + \frac{1}{\Lambda}[a-1]^2\lambda_+^3\int_{-\infty}^{0} g'([\xi+\phi]/\varepsilon)e^{c\xi}e^{2\lambda_+\xi}d\xi \\ &\approx \frac{1}{\Lambda}\left[a^2\lambda_-^3\int_0^{\infty} g'([\xi+\phi]/\varepsilon)d\xi + [a-1]^2\lambda_+^3\int_{-\infty}^{0} g'([\xi+\phi]/\varepsilon)d\xi\right] \\ &= \frac{\varepsilon}{\Lambda}(a\lambda_-)^2[\lambda_+-\lambda_-]g(\phi/\varepsilon)+\mathcal{O}(\varepsilon^2) \\ &= \frac{\varepsilon}{2[a-a^2]}g(\phi/\varepsilon)+\mathcal{O}(\varepsilon^2).\end{aligned}$$

Applying this to the sawtooth function (2.66), the phase Eq. (2.72) reduces to

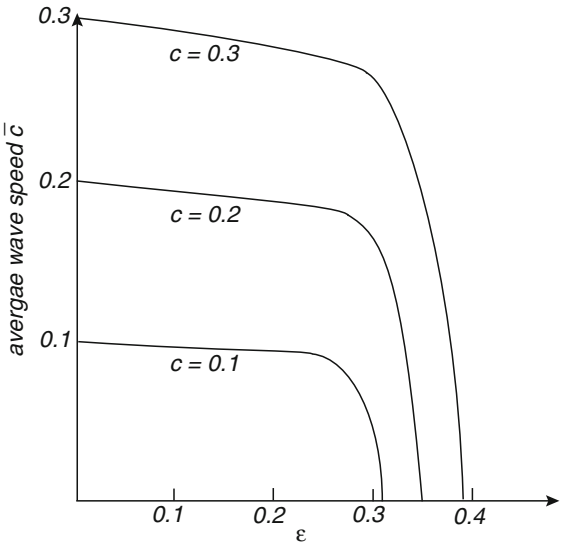

Fig. 2.11 Illustrative sketch of mean wave speed as a function of ε for the discrete bistable Eq. (2.65) with $L = 2\pi$

$$\frac{d\phi}{dt} = c - \frac{\varepsilon}{2[a-a^2]}\left[\frac{1}{2} - \frac{\phi}{\varepsilon}\right],$$

and

$$T = 2\ln\left(\frac{c+\varepsilon/\chi}{c-\varepsilon/\chi}\right), \quad \chi = 4[a-a^2].$$

We deduce that the mean wave speed is

$$\bar{c} = \frac{\varepsilon}{2}\frac{1}{\ln\left(\frac{c+\varepsilon/\chi}{c-\varepsilon/\chi}\right)}. \tag{2.82}$$

This predicts propagation failure when $\varepsilon \geq \chi c$. In particular, propagation failure is more likely to occur as ε increases, which is equivalent to reducing the coupling strength D. Finally, note that the cubic nonlinearity yields different behavior, both qualitatively and quantitatively. The main reason for this is that the above averaging procedure results in an expression for the mean wave speed that involves exponentially small terms of the form $e^{-\pi/\varepsilon}$ [318]. This has two major implications. First, it is necessary to include higher-order terms in the perturbation analysis in order to obtain sufficient accuracy. Second, the rapid increase in $e^{-\pi/\varepsilon}$ as ε increases can result in a sharp transition to propagation failure at relatively small values of ε, as illustrated in Fig. 2.11.

2.6 Stochastic Traveling Waves

In Sect. 1.5 we showed how the stochastic opening and closing of a finite number of ion channels can generate a multiplicative noise term in a space-clamped, conductance-based model of a neuron. The membrane voltage then evolves according to a stochastic differential equation (SDE) such as (1.128). This suggests that ion channel fluctuations could also affect the propagation of action potentials in a spatially extended model. Such an observation motivates the more general issue of how to analyze traveling wave solutions of stochastic partial differential equations (SPDEs). In this section we review a formal perturbation method for analyzing traveling front solutions in the case of weak noise [14, 494, 546, 557], which we apply to a stochastic version of the bistable equation. (The rigorous treatment of SPDEs is much more complicated than SDEs because one has to keep track of the regularity of solutions with respect to both time and space. Nevertheless, there have been some recent mathematical studies of a stochastic version of spatially extended excitable membranes based on the Hodgkin–Huxley equations [17, 88].)

Consider a scalar SPDE of the form

$$\frac{\partial}{\partial t}V(x,t)=\frac{\partial^2}{\partial x^2}V(x,t)+f(V(x,t))+\sqrt{\varepsilon}g(V(x,t))\eta(x,t), \tag{2.83}$$

Here $\eta(x,t)$ is a Gaussian random function with zero mean and correlation

$$\langle\eta(x,t)\eta(x',t')\rangle=2C([x-x']/\lambda)\delta(t-t') \tag{2.84}$$

The parameter λ is the spatial correlation length of the noise such that $C(x/\lambda)\to\delta(x)$ in the limit $\lambda\to 0$, and ε determines the strength of the noise, which is assumed to be weak. Note that we can formally set $\eta(x,t)dt=dW(x,t)$, where $W(x,t)$ is a space-dependent Wiener process with zero mean and $\langle dW(x,t)dW(x',t)\rangle=2C([x-x']/\lambda)$. We have also included a multiplicative noise factor $g(V)$, and based on our analysis of channel fluctuations, we treat the multiplicative noise in the sense of Stratonovich (see Sect. 1.7). The starting point of the perturbation method is the observation that multiplicative noise in the Stratonovich sense leads to a systematic shift in the speed of the front (assuming a front of speed c exists when $\varepsilon=0$) [14]. This is a consequence of the fact that $\langle g(V)\eta\rangle\neq 0$ even though $\langle\eta\rangle=0$. The former average can be calculated using Novikov's theorem [465, 486]:

$$\varepsilon^{1/2}\langle g(U)\eta\rangle=\varepsilon C(0)\langle g'(U)g(U)\rangle dt, \tag{2.85}$$

Note that in the limit $\lambda\to 0$, $C(0)\to 1/\Delta x$ where Δx is a lattice cutoff, which can be identified with the step size of the spatial discretization scheme used in numerical simulations.

Novikov's theorem. Suppose that $X(s)$ is a Gaussian random function with zero mean and correlation

$$\langle X(s)X(s')\rangle=C(s,s'),$$

then for any functional $\mathscr{L}[h]$,

$$\langle X(s)\mathscr{L}[X]\rangle = \int_{-\infty}^{\infty} C(s,s')\left\langle \frac{\delta \mathscr{L}[X]}{\delta X(s')}\right\rangle ds'.$$

Applying this theorem to $\langle g(U)\eta\rangle$, we have

$$\langle g(V)\eta\rangle = 2\int_{-\infty}^{\infty} C([x-x']/\lambda)\left\langle g'(V(x,t))\frac{\delta V(x,t)}{\delta \eta(x',t)}\right\rangle dx'.$$

The stochastic voltage is a functional of the noise term $\eta(x,t)$, as can be seen by formally integrating Eq. (2.83) with respect to time:

$$V(x,t) = \int_{-\infty}^{\infty}\left[\frac{\partial^2}{\partial x^2}V(x,t'') + f(V(x,t'')) + \sqrt{\varepsilon}g(V(x,t''))\eta(x,t'')\right]H(t-t'')dt''.$$

It follows that

$$\frac{\delta V(x,t)}{\delta \eta(x',t')} = \sqrt{\varepsilon}g(V(x,t'))H(t-t')\delta(x-x'),$$

which yields (2.85) after using $H(0) = 1/2$.

An alternative derivation of (2.85) is based on Fourier transforming (2.83) [546]. It is convenient to restrict x to a bounded domain, $-L/2 \le x \le L/2$, and to impose periodic boundary conditions. We can then introduce the discrete Fourier series

$$V(x,t) = \frac{1}{L}\sum_n \mathrm{e}^{ik_n x}V_n(t), \quad W(x,t) = \frac{1}{L}\sum_n \mathrm{e}^{ik_n x}W_n(t) \tag{2.86}$$

with $k_n = 2\pi n/L$ and $W_n(t)$, an independent Wiener process, such that

$$\langle dW_n(t)\rangle = 0, \quad \langle dW_n(t)dW_m(t)\rangle = 2L\delta_{m+n,0}dt. \tag{2.87}$$

Fourier transforming (2.83) gives in differential form

$$dU_n(t) = [-k_n^2 V_n(t) + F_n(t)]dt + \frac{\varepsilon^{1/2}}{L}\sum_m g_{n-m}(t)dW_m(t), \tag{2.88}$$

where F_n, g_n are the Fourier coefficients of the time-dependent functions $F\circ U(t)$ and $g\circ U(t)$, respectively. The associated Stratonovich Fokker–Planck equation takes the form [209] (see also Sect. 1.7)

$$\frac{\partial P}{\partial t} = -\sum_l \frac{\partial}{\partial u_l}[(-k_l^2 V_n(t) + F_l(t))P] + \frac{\varepsilon}{L}\sum_{l,m,q}\frac{\partial}{\partial V_l}g_{l-q}\frac{\partial}{\partial V_m}g_{m+q}P. \tag{2.89}$$

Multiplying both sides of this equation by V_n and integrating with respect to V_m, integer m, leads to the following evolution equation for the mean:

$$\frac{d\langle V_n\rangle}{dt} = -k_n^2\langle V_n\rangle + \langle F_n\rangle + \frac{\varepsilon}{L}\sum_{m,q}\left\langle \frac{\partial g_{n-q}}{\partial V_m}g_{m+q}\right\rangle. \tag{2.90}$$

Finally, taking the inverse transform of (2.90) gives

$$\frac{d\langle U(x,t)\rangle}{dt} = \frac{\partial^2}{\partial x^2}\langle V(x,t)\rangle + \langle F(V(x,t))\rangle + \frac{\varepsilon}{\Delta x}\left\langle g(U(x,t))g'(U(x,t))\right\rangle, \tag{2.91}$$

where we have used the result $\partial g_n/\partial U_m = [g'(U)]_{n-m}$. Note that it is necessary to introduce a cutoff in the frequencies, which is equivalent to introducing a fundamental lattice spacing of Δx. Alternatively, the multiplicative noise can be taken to have a small but finite corre-

lation length in space so that $C(0) = 1/\Delta x$. Comparison of (2.90) with the mean of (2.83) yields the desired result.

Following [14], it is convenient to rewrite (2.83) so that the fluctuating term has zero mean:

$$\frac{\partial}{\partial t}V(x,t) = \frac{\partial^2}{\partial x^2}V(x,t) + h(V(x,t)) + \sqrt{\varepsilon}R(V,x,t), \tag{2.92}$$

where

$$h(V) = f(V) + \varepsilon C(0)g'(V)g(V) \tag{2.93}$$

and

$$R(V,x,t) = g(V)\eta(x,t) - \varepsilon^{1/2}C(0)g'(U)g(U). \tag{2.94}$$

The stochastic process R has zero mean (so does not contribute to the effective wave speed) and correlation:

$$\langle R(V,x,t)R(V,x',t')\rangle = \langle g(V(x,t))\eta(x,t)g(V(x',t')\eta(x',t')\rangle + \mathscr{O}(\varepsilon^{1/2}). \tag{2.95}$$

The next step in the analysis is to assume that the fluctuating term in (2.92) generates two distinct phenomena that occur on different time scales: a diffusive-like displacement of the front from its uniformly translating position at long time scales and fluctuations in the front profile around its instantaneous position at short time scales [14, 494, 546, 557]. In particular, following [14], we express the solution V of (2.92) as a combination of a fixed wave profile V_0 that is displaced by an amount $\Delta(t)$ from its uniformly translating position $\xi = x - \bar{c}t$ and a time-dependent fluctuation Φ in the front shape about the instantaneous position of the front:

$$V(x,t) = V_0(\xi - \Delta(t)) + \varepsilon^{1/2}\Phi(\xi - \Delta(t),t). \tag{2.96}$$

The wave profile V_0 and associated wave speed $\bar{c}$ are obtained by solving the modified deterministic equation

$$\bar{c}\frac{dV_0}{d\xi} + \frac{d^2V_0^2}{d\xi^2} + h(V_0(\xi)) = 0. \tag{2.97}$$

Both $\bar{c}$ and V_0 depend nontrivially on the noise strength ε due to the ε dependence of the function h; see (2.93). As an example, suppose that $f(V) = V(V-a)(1-V)$ and $g(V) = V(1-V)$ [14]. The form of multiplicative noise is chosen so that it preserves the stationary states $V = 0, 1$. Hence, the noise is most important in regions close to the front but vanishes asymptotically at $\xi \pm \infty$. The effective nonlinearity h is also a cubic with

$$h(V) = V(1-V)(a' - k'V), \quad a' = a - \varepsilon C(0), \quad k' = 1 - 2\varepsilon C(0).$$

Thus, from the analysis of the bistable equation in Sect. 2.2, we find that $\bar{c} = (k' - 2a')/\sqrt{2k'}$.

It turns out that if V_0 is chosen to satisfy (2.97) then to leading order, the stochastic variable $\Delta(t)$ undergoes unbiased Brownian motion (a Wiener process):

$$\langle \Delta(t) \rangle = 0, \quad \langle \Delta(t)^2 \rangle = 2D(\varepsilon)t \tag{2.98}$$

with a diffusion coefficient $D(\varepsilon) = \mathscr{O}(\varepsilon)$ (see below). Thus $\Delta(t)$ represents the effects of slow fluctuations, whereas Φ represents the effects of fast fluctuations. Note that since $\Delta(t) = \mathscr{O}(\varepsilon^{1/2})$, (2.96) implies that $V(x,t) = V_0(x-\bar{c}t) + \mathscr{O}(\varepsilon^{1/2})$. Hence, averaging with respect to the noise shows that $\langle V(x,t) \rangle = V_0(x-\bar{c}t) + \mathscr{O}(\varepsilon^{1/2})$. Thus, in the case of weak noise, averaging over many realizations of the stochastic wave front generates a mean front whose speed is approximately equal to $\bar{c}$.

Calculation of diffusion coefficient. Substitute the decomposition (2.96) into (2.92) and expand to first order in $\mathscr{O}(\varepsilon^{1/2})$ (exploiting the fact that the usual rules of calculus apply in the case of Stratonovich noise, see Sect. 1.7):

$$\begin{aligned} &-[\bar{c}+\dot{\Delta}(t)]V_0'(\xi_t) + \varepsilon^{1/2}\left[\partial_t \Phi(\xi_t,t) - [\bar{c}+\dot{\Delta}(t)]\partial_\xi \Phi(\xi_t,t)\right] \\ &\quad = h(V_0(\xi_t) + \varepsilon^{1/2} h'(V_0(\xi_t))\Phi(\xi_t,t) \\ &\quad +\partial_\xi^2 \left[V_0(\xi_t) + \varepsilon^{1/2}\Phi(\xi_t,t)\right] + \varepsilon^{1/2} R(V_0(\xi_t),x,t) + \mathscr{O}(\varepsilon), \end{aligned}$$

where $\xi_t \equiv \xi - \Delta(t)$. Imposing (2.97) and dividing through by $\varepsilon^{1/2}$ then gives

$$\frac{\partial \Phi(\xi,t)}{\partial t} + \mathbb{L}_\xi \Phi(\xi,t) = \varepsilon^{-1/2} V_0'(\xi)\dot{\Delta}(t) + R(V_0(\xi),\xi,t) + \mathscr{O}(\varepsilon^{1/2}), \tag{2.99}$$

where $\mathbb{L}_\xi$ is the non-self-adjoint linear operator

$$\mathbb{L}_\xi A(\xi) = A''(\xi) + \bar{c}A'(\xi) + h'(V_0(\xi))A(\xi) \tag{2.100}$$

for any function $A(\xi) \in L^2(\mathbb{R})$. We have also made the approximation $\xi_t \approx \xi$, since $\Delta(t) = \mathscr{O}(\varepsilon^{1/2})$. The linear differential operator $\mathbb{L}_\xi$ has a zero eigenvalue with associated eigenfunction $V_0'(\xi)$, which can be seen by differentiating (2.97) with respect to ξ, and reflects the fact that the underlying system is equivariant with respect to uniform translations. We then have the solvability condition for the existence of a bounded solution of (2.99), namely, that the inhomogeneous part on the right-hand side is orthogonal to all elements of the null-space of the adjoint operator $\mathbb{L}_\xi^\dagger$. The latter is defined with respect to the inner product

$$\int_{-\infty}^{\infty} B(\xi)\mathbb{L}_\xi A(\xi) d\xi = \int_{-\infty}^{\infty} \left[\mathbb{L}_\xi^\dagger B(\xi)\right] A(\xi) d\xi \tag{2.101}$$

where $A(\xi)$ and $B(\xi)$ are arbitrary integrable functions. Hence,

$$\mathbb{L}_\xi^\dagger B(\xi) = B''(\xi') - \bar{c}B'(\xi) + h'(V_0(\xi))B(\xi). \tag{2.102}$$

The linear operator $\mathbb{L}^\dagger$ also has a zero eigenvalue, with corresponding eigenfunction $\mathscr{V}(\xi) = \mathrm{e}^{\bar{c}\xi}V_0'(\xi)$. Thus taking the inner product of both sides of (2.99) with respect to $\mathscr{V}(\xi)$ leads to the solvability condition

$$\int_{-\infty}^{\infty} \mathscr{V}(\xi)\left[V_0'(\xi)\dot{\Delta}(t) + \varepsilon^{1/2} R(V_0,\xi,t)\right] d\xi = 0, \tag{2.103}$$

which implies that $\Delta(t)$ satisfies the stochastic differential equation (SDE)

$$d\Delta(t) = -\varepsilon^{1/2} \frac{\int_{-\infty}^{\infty} \mathscr{V}(\xi) dR(V_0, \xi, t) d\xi}{\int_{-\infty}^{\infty} \mathscr{V}(\xi) V_0'(\xi) d\xi}. \tag{2.104}$$

Using the lowest-order approximation $dR(V_0, \xi, t) = g(V_0(\xi))dW(\xi, t)$, we deduce that (for $\Delta(0) = 0$) $\Delta(t)$ is a Wiener process with diffusion coefficient

$$D(\varepsilon) = \varepsilon \frac{\int_{-\infty}^{\infty} \int_{-\infty}^{\infty} \mathscr{V}(\xi) \mathscr{V}(\xi') g(V_0(\xi)) g(V_0(\xi')) C([\xi - \xi']/\lambda) d\xi d\xi'}{\left[\int_{-\infty}^{\infty} \mathscr{V}(\xi) V_0'(\xi) d\xi \right]^2}. \tag{2.105}$$

Although the above analysis is based on a formal perturbation calculation, rather than rigorous analysis, it does appear to capture well the effects of weak external noise on front propagation in a variety of reaction–diffusion models [486, 546]. In Sect. 7.4, we will show how the method can be extended to study stochastic traveling waves in nonlocal neural field equations, which represent large-scale continuum models of spatially structured neural networks. Note, however, that one class of front solution where the method breaks down is a so-called pulled front, which propagates into an unstable rather than a metastable state and whose dynamics is dominated by the linear spreading of small perturbations within the leading edge of the front [544]. One well-known reaction–diffusion model that supports pulled fronts is the Fisher–KPP equation [191, 345]. As we will describe later, pulled fronts also arise in a PDE model of CaMKII translocation waves along spiny dendrites [72, 161] (Sect. 3.2), in certain neural field models (Sect. 7.4), and in a model of protein aggregation (Sect. 9.6).

2.7 Appendix: Linear Differential Operators

Throughout this book, we will encounter linear operators acting on some function space. As already demonstrated in this chapter, linear differential operators arise when analyzing the stability of a traveling wave solution of some PDE, or when carrying out a formal perturbation expansion. In this appendix, we summarize some of the basic results regarding linear differential operators acting on a function space, viewed from the perspective of a linear map acting on an infinite-dimensional vector space. For simplicity, we will restrict ourselves to real-valued functions $f : \mathbb{R} \to \mathbb{R}$, although it is straightforward to generalize the results to complex-valued functions.

2.7.1 Function Spaces

Consider the set of all real functions $f(x)$ on the interval $[a, b]$. This is a vector space over the set of real numbers: given two functions $f_1(x), f_2(x)$ and two real

numbers a_1, a_2, we can form the sum $f(x) = a_1 f_1(x) + a_2 f_2(x)$ such that $f(x)$ is also a function on $[a,b]$. Either on physical grounds or for mathematical convenience, we usually restrict ourselves to a subspace of functions that are differentiable to some given order. For example, the space of functions on $[a,b]$ with n continuous derivatives is denoted by $C^n[a,b]$, and the space of analytic functions (those whose Taylor expansion converges to the given function) is denoted by $C^\omega[a,b]$.

In order to describe the convergence of a sequence of functions $f_n, n = 1,2,\ldots$ to a limit function f, we need to introduce the concept of a *norm*, which is a generalization of the usual measure of the length of a finite-dimensional vector. The norm $\|f\|$ of a function f is a real number with the following properties:

(i) Positivity: $\|f\| \geq 0$, and $\|f\| = 0$ if and only if $f = 0$
(ii) The triangle inequality: $\|f+g\| \leq \|f\| + \|g\|$
(iii) Linearity: $\|\lambda f\| = |\lambda| \|f\|$ for $\lambda \in \mathbb{R}$

Common examples of norms are the "sup" norm

$$\|f\|_\infty = \sup_{x\in[a,b]} |f(x)|,$$

and the L^p norm

$$\|f\|_p = \left(\int_a^b |f(x)|^p dx \right)^{1/p}.$$

Given the L^p norm, we can introduce another important function space $L^p[a,b]$, which is the space of real-valued functions on $[a,b]$ for which $\|f\|_p < \infty$. However, there is one subtlety here, namely, that it is possible for $\|f\| = 0$ without f being identically zero. For example, f may vanish at all but a finite set of points (set of measure zero). This violates the positivity property of a norm. Therefore, one should really treat elements of $L^p[a,b]$ as equivalence classes of functions, where functions differing on a set of measure zero are identified.

Given a normed function space, convergence of a sequence $f_n \to f$ can be expressed as

$$\lim_{n\to\infty} \|f_n - f\| = 0.$$

In the case of the "sup" norm, f_n is said to converge *uniformly* to f, whereas for the L^1 norm, it is said to converge *in the mean*. An important property of a function space is that of being *complete*. First, consider the following definition of a *Cauchy sequence*: A sequence f_n in a normed vector space is Cauchy if for any $\varepsilon > 0$, we can find an integer N such that $n, m > N$ implies that $\|f_m - f_n\| < \varepsilon$. In other words, elements of the sequence become arbitrarily close together as $n \to \infty$. A normed vector space is then *complete* with respect to its norm if every Cauchy sequence converges to some element in the space. A complete normed vector space is called a Banach space $\mathscr{B}$. In many applications, the norm of the function space is taken to be the so-called natural norm obtained from an underlying *inner product*. For example, if we define an inner product for $L^2[a,b]$ according to

$$\langle f,g\rangle = \int_a^b f(x)g(x)dx,$$

then the $L^2[a,b]$ norm can be written as

$$\|f\|_2 = \sqrt{\langle f,f\rangle}.$$

A Banach space with an inner product is called a *Hilbert space* $\mathscr{H}$.

2.7.2 Fredholm Alternative Theorem

In the case of one-dimensional traveling wave solutions, it is more natural to consider functions on the real line $\mathbb{R}$ rather than a finite interval. Suppose that $\mathbb{L}$ is a linear differential operator acting on a subspace of $L^2(\mathbb{R})$, which we denote by the domain $\mathscr{D}(\mathbb{L})$. Linearity of the operator means that for $f_1, f_2 \in \mathscr{D}(\mathbb{L})$ and $a_1, a_2 \in \mathbb{R}$,

$$\mathbb{L}(a_1 f_1 + a_2 f_2) = a_1 \mathbb{L} f_1 + a_2 \mathbb{L} f_2.$$

Given the standard inner product on $L^2(\mathbb{R})$, we define the adjoint linear operator $\mathbb{L}^\dagger$ according to

$$\langle f, \mathbb{L} g\rangle = \langle \mathbb{L}^\dagger f, g\rangle, \quad f,g \in \mathscr{D}(L).$$

The operator is said to be self-adjoint if $\mathbb{L}^\dagger = \mathbb{L}$. Note that, in practice, one determines $\mathbb{L}^\dagger$ using integration by parts. For functions defined on finite intervals, this generates boundary terms that only vanish if appropriate boundary conditions are imposed. In general, this can result in different domains for $\mathbb{L}$ and $\mathbb{L}^\dagger$. Therefore, the condition for self-adjointness becomes $\mathbb{L} = \mathbb{L}^\dagger$ and $\mathscr{D}(\mathbb{L}) = \mathscr{D}(\mathbb{L}^\dagger)$. Given a differential operator $\mathbb{L}$ on $L^2(\mathbb{R})$, we can now state the *Fredholm alternative theorem*: The inhomogeneous equation

$$\mathbb{L} f = h$$

has a solution if and only if

$$\langle h, v\rangle = 0 \quad \text{for all v satisfying} \quad \mathbb{L}^\dagger v = 0.$$

2.7.3 Spectrum of a Linear Differential Operator

Let $\mathscr{B}$ be a Banach space and $\mathbb{L} : \mathscr{D}(\mathbb{L}) \to \mathscr{B}$ be a linear operator with domain $\mathscr{D}(\mathbb{L}) \subseteq \mathscr{B}$. For any complex number λ, introduce the new operator

$$\mathbb{L}_\lambda = \mathbb{L} - \lambda \mathbb{I},$$

where $\mathbb{I}$ is the identity operator on $\mathscr{B}$. If $\mathbb{L}_\lambda$ has an inverse, then $R_\lambda(\mathbb{L}) = \mathbb{L}_\lambda^{-1}$ is called the resolvent of $\mathbb{L}$. Given these definitions, λ is said to be a regular point for $\mathbb{L}$ if the following hold:

(i) R_λ exists.
(ii) R_λ is bounded.
(iii) R_λ is defined on a dense subset of $\mathscr{B}$.

The spectrum $\sigma(\mathbb{L})$ is then the set of points that are not regular, which generally consists of three disjoint parts:

(a) The *point spectrum* of eigenvalues is the set of values of λ for which R_λ does not exist.
(b) The *continuous spectrum* is the set of values of λ for which R_λ exists but is unbounded.
(c) The *residual spectrum* is the set of values of λ for which R_λ exists, is bounded, but is not defined on a dense subset of $\mathscr{B}$.

The continuous spectrum and residual spectrum are contained in the essential spectrum, which is any point in $\sigma(\mathbb{L})$ that is not an isolated eigenvalue of finite multiplicity.

We will illustrate how to calculate the essential spectrum of a simple linear operator acting on $\mathscr{B} = L^2(\mathbb{R})$ [242]:

$$\mathbb{L}u = u_{xx} + pu_x - qu \tag{2.106}$$

for constant positive coefficients p, q and $\mathscr{D}(\mathbb{L}) = \{u : u \in L^2(\mathbb{R}), \mathbb{L}u \in L^2(\mathbb{R})\}$. Firstly, suppose that $\mathbb{L}_\lambda$ is not invertible for some λ. This means that there exists $\phi \in \mathscr{B}$ such that $\mathbb{L}_\lambda \phi = 0$. The latter equation is a linear second-order ODE with constant coefficients and thus has solutions of the form $e^{\nu_\pm x}$ with $\nu_\pm$, the roots of the characteristic polynomial $\nu^2 + p\nu - (q+\lambda) = 0$. Such a solution cannot decay at both $x = \pm\infty$ and so does not belong to $\mathscr{B}$. It follows that $\mathbb{L}$ has no eigenvalues and the resolvent R_λ exists. We can then represent R_λ in terms of the Green's function G defined according to $\mathbb{L}_\lambda^\dagger G(x-x') = \delta(x-x')$, where $\mathbb{L}^\dagger$ is the adjoint of $\mathbb{L}$ with respect to the standard inner product on $L^2(\mathbb{R})$:

$$\mathbb{L}_\lambda^\dagger u = u_{xx} - pu_x - (q+\lambda)u.$$

For any $h \in \mathscr{D}(R_\lambda) \subseteq \mathscr{B}$ we can express the solution $u = R_\lambda h$ to the inhomogeneous equation $\mathbb{L}_\lambda u = h$ as

$$u(x) = \int_{-\infty}^{\infty} h(y)G(y-x)dy.$$

For constant coefficients, the Green's function can be solved explicitly according to

$$G(y) = \begin{cases} \alpha e^{\mu_+ y} & y \le 0 \\ \alpha e^{\mu_- y} & y \ge 0, \end{cases}$$

where $\mu_\pm$ are the roots of the characteristic polynomial

$$P(\mu) = \mu^2 - p\mu - (\lambda + q),$$

and α is chosen such that $-1 = \alpha(\mu_+ - \mu_-)$.

If $P(\mu)$ has one root μ_+ with positive real part and one root μ_- with negative real part, then clearly $G \in L_1(\mathbb{R})$ so that R_λ is bounded with dense domain equal to $\mathscr{B}$. This situation holds, for example, when λ is real and $\lambda > -p$. The roots of $P(\mu)$ vary continuously with λ in the complex plane. Hence, the boundedness of R_λ will break down when one of the roots crosses the imaginary axis at ik, say, with $\lambda = -q - k^2 - ika$. This is a parabola in the complex λ plane (λ_r, λ_i) given by $\lambda_r = -q - \lambda_i^2/p^2$. If λ_r is to the right of this parabola,

$$\lambda_r > -q - \frac{\lambda_i^2}{p^2},$$

then $P(\mu)$ has a root on either side of the imaginary axis and R_λ is bounded. We conclude that the essential spectrum lies to the left of the parabola,

$$\sigma(\mathbb{L}) \subseteq \{\lambda : \mathrm{Re}(\lambda) \leq -q - \mathrm{Im}(\lambda)^2/p^2\}. \tag{2.107}$$

It can be shown that the essential spectrum includes the parabola itself. It immediately follows that the essential spectrum lies in the left-half complex plane if $q > 0$.

In Sect. 2.4, we considered the linear stability of a traveling front, which required finding the spectrum of a second-order linear operator with nonconstant coefficients; see (2.42). It turns out that one can generalize the above analysis to an operator with x-dependent coefficients $p(x), q(x)$. Suppose that $p(x), q(x) \to p_\pm, q_\pm$ as $x \to \pm\infty$. Introduce the parabolas

$$S_\pm = \{\lambda : \lambda = -q_\pm - k^2 - ikp_\pm\}. \tag{2.108}$$

Let A denote the union of the regions to the left of the curves $S_\pm$ that includes the curves themselves. Then the essential spectrum of $\mathbb{L}$ lies in A and includes $S_\pm$.